Summer 2018

Reprocessing of 3C-2D seismic reflection data from the Spring Coulee Field, Alberta

Yasin Demir

REPROCESSING OF 3C-2D SEISMIC REFLECTION DATA FROM THE SPRING COULEE FIELD, ALBERTA

by

YASIN DEMIR

A THESIS

Presented to the Graduate Faculty of the

MISSOURI UNIVERSITY OF SCIENCE AND TECHNOLOGY

In Partial Fulfillment of the Requirements for the Degree

MASTER OF SCIENCE

in

GEOLOGY AND GEOPHYSICS

2018

Approved by

Dr. Kelly Liu, Advisor
Dr. Stephan Gao
Dr. Neill Anderson

ABSTRACT

The 3C-2D seismic datasets were acquired in 2008 in the Spring Coulee Field, Alberta, which is located in Township 4, Range 23, and west of the 4th Meridian in the Alberta Basin. Line 2008-SC-01 was reprocessed to obtain better image of the formation targeted at between 1300 ms and 1400 ms. The depositional settings of the Madison Formation consist of shallow and carbonate shelf deposits. The processing workflow was designed by testing several methods, algorithms, and parameters, and finding the optimal processing solution. The processing steps included elevation statics, noise suppression, deconvolution operator, and 2D Kirchhoff poststack time migration. In order to obtain the high quality seismic section, noise suppressing is important for this study because data include high ground rolls and air blast noises. Therefore, the recorded effects of ground roll and air blast were suppressed using suppress module, F-K, and bandpass filters. The final seismic section provides a high quality imaging of the subsurface. Combining the results of the reprocessed seismic data with well data from the same area allows for seismic interpretation and hydrocarbon exploration.

ACKNOWLEDGMENTS

I would like to thank Dr. Kelly Liu for her suggestions and positive reinforcement during my study. I also thank Dr. Stephan Gao and Dr. Neil Anderson for being members of the Master Thesis Committee.

I am really grateful to my sponsors, Turkish Petroleum Corporation (TPAO), and Turkish Ministry of National Education for providing me this opportunity to pursue a master degree in the USA.

I am thankful to my mother and my father for their support, Atalay Demir and Dilara Demir. They are always there for me during my life.

Thank you to all my friends and relatives, who shared their support and motivation.

TABLE OF CONTENTS

Page

LIST OF ILLUSTRATIONS

LIST OF TABLES

1. INTRODUCTION

The 3C-2D seismic datasets used in this study were acquired in 2008 through the CREWES Project by University of Calgary in the Spring Coulee Field, Alberta. The survey area is located in Township 4, Range 23, and west of the 4th Meridian in the Alberta Basin (Figure 1.1) (Lu and Hall, 2008).

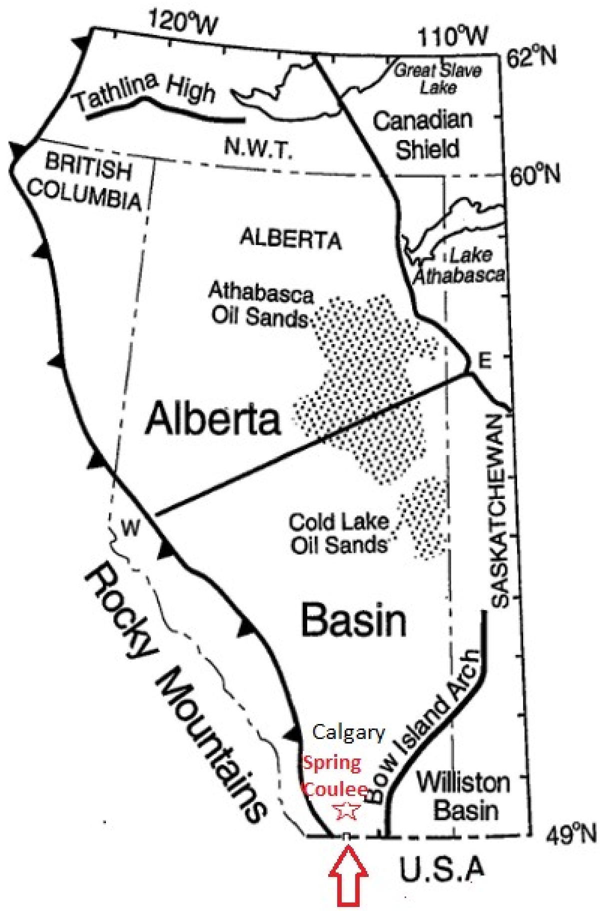

Figure 1.1. Map of the Alberta Basin and the study area (modified from Liu et al., 1997).

There was no oil and gas production in the survey area. The purpose of the survey is to analyze the hydrocarbon potential of the survey area. Different types of sources and receivers were used to compare the effect on the seismic data from the various sources and receivers (Bertram et al., 2008).

Location of Line 2008-SC-01 used in this study is shown in Figure 1.2. SM7 analog sensor was utilized with the ARAM recording systems. The source was two Mertz Hemi vibes. The length of the survey line was 6.5 km (Bertram et al., 2008).

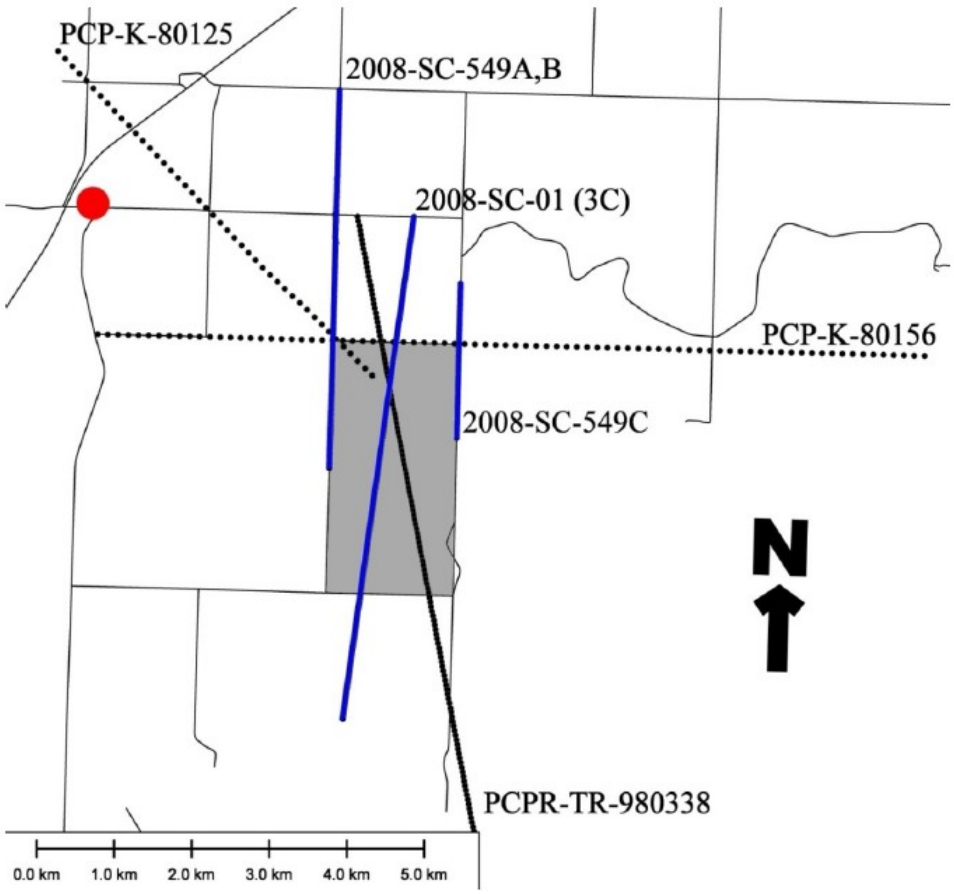

Figure 1.2. Location of Line 2008-SC-01 (Lu and Hall, 2008).

The main purpose of this study is to reprocess Line 2008-SC-01 to enhance the image of the target zone, which is the Madison Formation between 1300 ms and 1400 ms. The Madison Formation has a potential of finding hydrocarbons in the target sandstone reservoirs and neighboring shales (Lauren and Stewart,2008).

1.1. GEOLOGICAL BACKGROUND

The western Canadian sedimentary basin contains the eastern Canadian Cordillera, Alberta Basin, and Williston Basin (Wright et al., 1994). The Spring Coulee Field is located in the Alberta Basin (Figure 1.3). The Alberta Basin is bordered by the Rock Mountain Thrust Belt to the west, and the Williston Basin to the southeast (Liu et al., 1997). The basin is a simple monocline structure consisting of unreformed, northwestern trending Paleozoic and Mesozoic sediment rocks (Connolly et al., 1990).

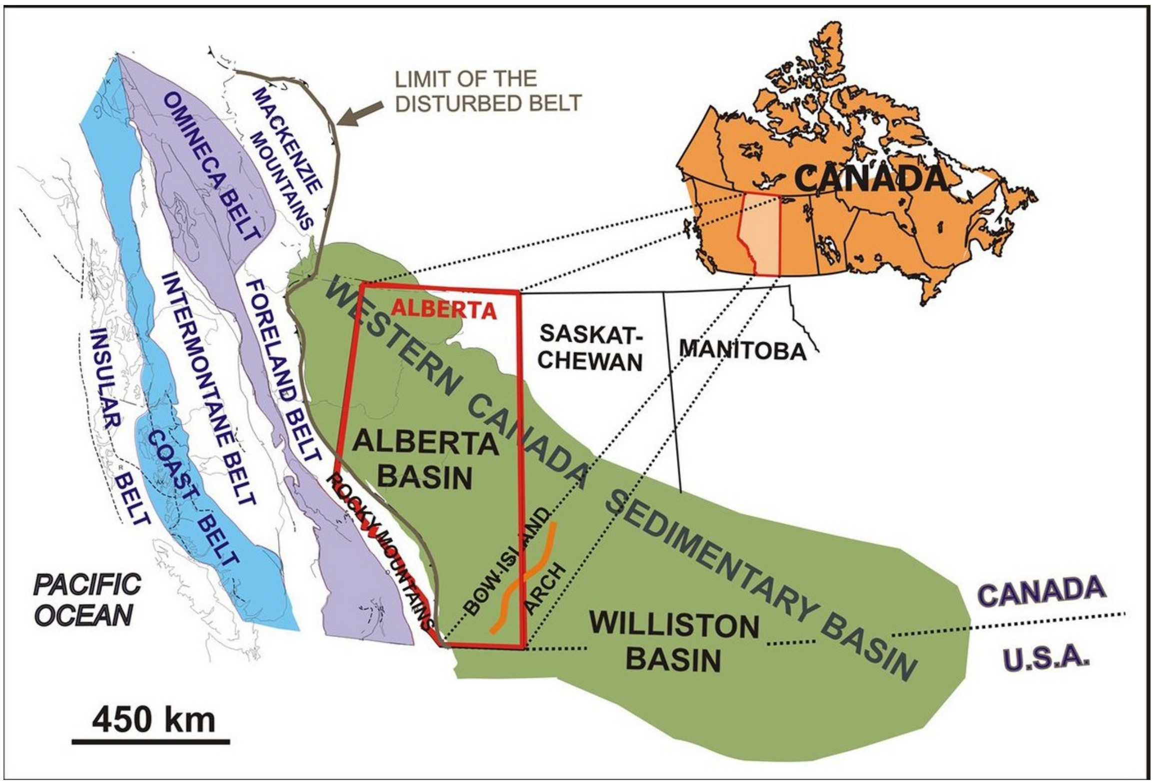

Figure 1.3. Location of the Alberta Basin (Garland et al., 2012).

The study area is unexplored, and no well was drilled. Therefore, analyzing the hydrocarbon potential of the study area is challenging. However, there are two wells nearby the study area. Well 3-32 produces from the Madison Formation of the Mississippian age, which is approximately 10 miles to the south. Well 4-34 produces from the Second White

Speckled Shale of Createaceous age, which is about 80 miles to the southeast (Lauren and Stewart, 2008). Therefore, Well 3-32 is useful to understand the geological structure of the area.

The hydrocarbon potential of the area is evaluated and concluded with that there is a possibility to find petroleum in the zone of interest. The Madison Formation was deposited on a shallow and carbonate shelf. Thus, the formation has a potential to be a good reservoir due to dolomitization, fractures, and structure caused by tectonic movement (Lauren and Stewart, 2008). The Paleozoic strata are approximately 870 m thick, and the Madison Formation is roughly 150 m. Mississippian rocks are generally carbonates and, the youngest rocks of carbonates occur in the Mississippian Madison Formation (Kent and Kreis, 2001) (Figure 1.4). Also, shale formation is observed in the deeper Mississippian (Ostridge et al., 2009).

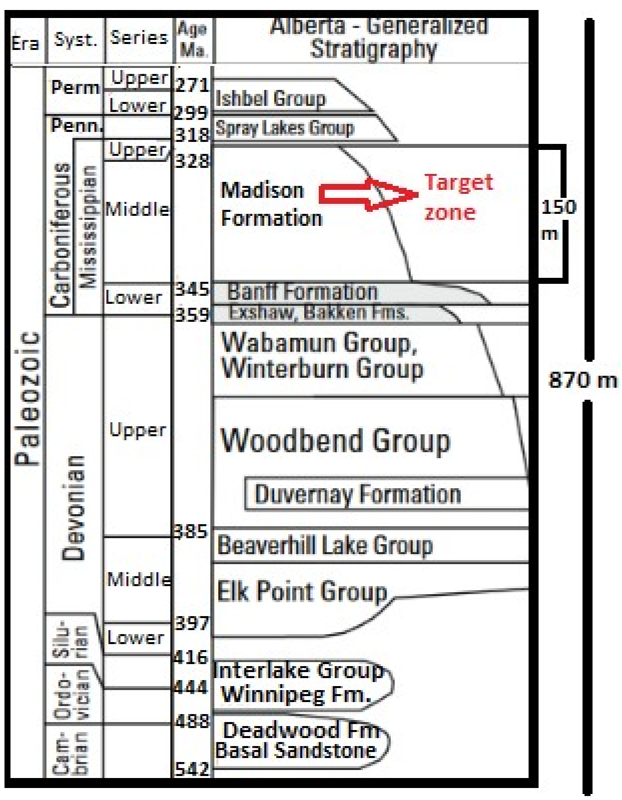

Figure 1.4. Stratigraphic formations in the Spring Coulee Field (modified from Higley, 2013).

1.2. GENERAL OVERVIEW OF LAND DATA ACQUISITION

In general, a seismic acquisition system constitutes the source such as dynamite, vibroseis, hammer, etc., receivers, recorder, gain controller, A/D converter, tape driver, and cable (Figure 1.5). Data acquisitions are conducted as 2D and 3D surveys. They are preferred with respect to survey purpose and cost. Geophones are alligned in the same line. However, sources may not be in the same order for 2D surveys (Evans and Dragoset, 1997).

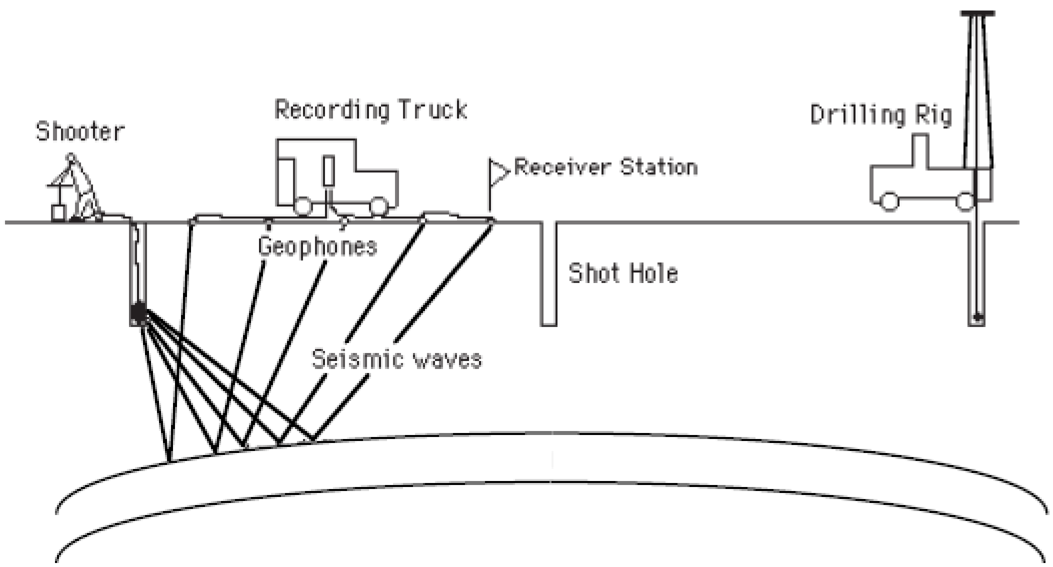

Figure 1.5. Seismic data acquisition operation system with an exploisve source (Evans and Dragoset, 1997).

1.2.1. Sources. For land seismic data acquisition, different types of sources such as explosive sources (dynamite and air gun) and non explosive sources (vibroseis) are used. Also, they produce generally compressional waves which play a key role for seismic surveying. They are differ in energy levels and frequency characteristics (Figure 1.6). The frequency content ranges from 1 Hz to several hundred Hz. The most popular sources used for seismic survey are vibroseis and dynamite (Kearey et al., 2013).

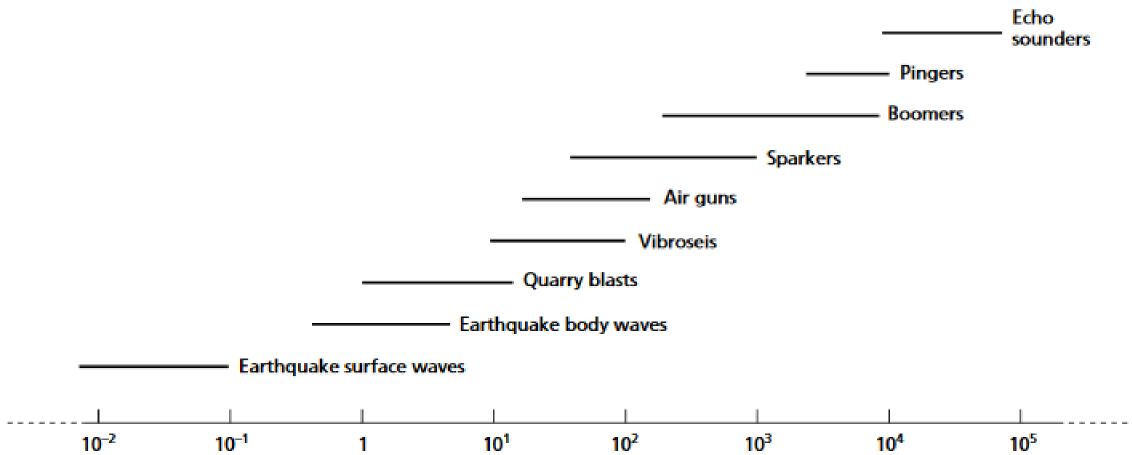

Figure 1.6. Frequency ranges for seismic sources (Kearey et al., 2013).

Vibroseis, invented by Conoco, is the most common method among non-explosive sources. Sweep signal, known as low amplitude and continuously varying frequency, is produced by vibroseis. The frequency band limits between 10 and 80 Hz. The obtained seismic trace from field recording includes low amplitude signal obscured by ambient noise. Therefore, to improve signal-to-noise ratio and also shorten the pulse length, cross-correlation is implemented (Figure 1.7). After the cross-correlation, the seismogram appears similar to the seismogram obtained from explosive source, and the produced signal wavelet is zero phase (Kearey et al., 2013).

Dynamite is an impulsive source. This results an impulsive source with a wide bandwidth. Also, the wavelet type is a minimum phase. Gelatin dynamite and ammonium nitrate are used as an explosive for seismic surveys (Sheriff and Geldart, 1983).

The significant difference between vibroseis and dynamite is that frequency can be controlled in vibroseis method, and this provides improved signal to noise ratio in areas where surface waves are a problem (Costain and Çoruh, 2004). Although dynamite provides high energy sources, it has several disadvantages such as high cost, damage to nature and

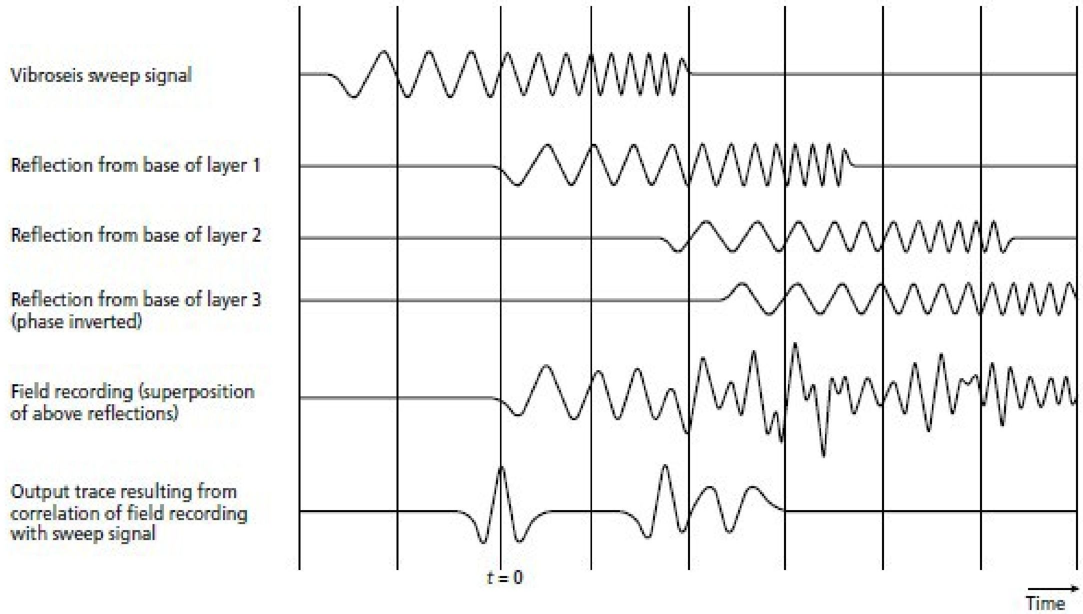

Figure 1.7. Cross-correlation section (Kearey et al., 2013).

buildings, needing wells, time etc. On the other hand, vibroseis source is quick, repeatable, and not harmful for environment. Vibroseis can be used in towns; however, using dynamite in towns is not possible (Kearey et al., 2013).

1.2.2. Receivers. Receivers are used to convert a mechanical input (the seismic pulse) into an electrical output. On land surveys, they are known as seismometers or geophones to detect seismic ground motions. Modern geophones are generally moving-coil electromagnetic type. Geophones, preferred in accordance with the purpose of survey have natural frequency from 1 Hz to 60 Hz. 4-15 Hz geophones are used for oil exploration reflection method (Sheriff and Geldart,1983).

Working principle of typical geophones is related to vertical movement, but they cannot give an output for horizontal movement. Thus, several type of special geophones (shear geophone, gimballed geophone, and three-component geophone) were upgraded by manufacturers. Shear wave geophones can be used to detect horizontal movements. Also, gimballed geophone has the same principle as the shear geophone, but the difference is that it performs well at tilt angles up to 30 degree (Evans and Dragoset, 1997). The three-component geophone includes X, Y, and Z components. The Z component is able to acquire P-wave, while the X component and Y component can obtain S-wave. As a result, P-wave and S-wave can be received by the three-component geophone (Zhang et al., 2017) (Figure 1.8).

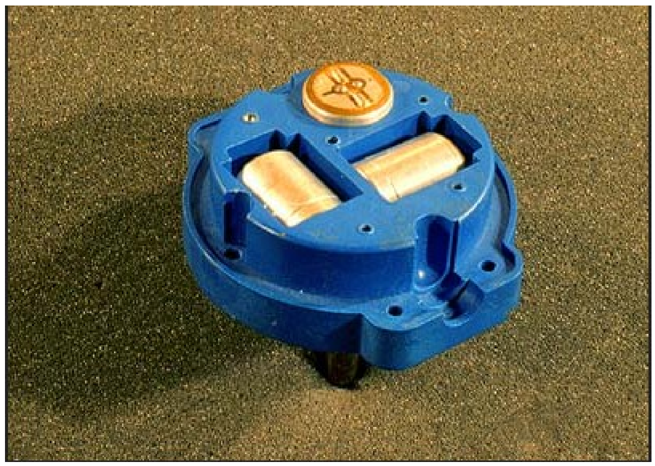

Figure 1.8. Three-component geophone (Kearey et al., 2013).

1.3. SURVEY ACQUISITION

The 3C-2D is to use conventional source to acquire the 2D data recorded on 3C geophone. The survey has two main purposes, which include to compare 3C geophone data to MEMS accelerometer data and to investigate development potential of the survey area. In this survey, different sources and receivers are used in the 2-D seismic lines (Figure 1.9). Three different receivers, which are SM7, SM24, and Sercel DSU3 respectively, are used in order to obtain a true comparision of the sensors for signal-to-noise ratio and sensitivity (Bertram et al., 2008).

Line 1 starts with station 101 in the north and ends with station 752 in the south. Receiver spacing is 10 m, and a three-component Sensor SM7 geophone and a Sercel DSU3 MEMS accelerometer are placed about 0.5 m apart at each stations (Bertram et al., 2008) (Figure 1.10).

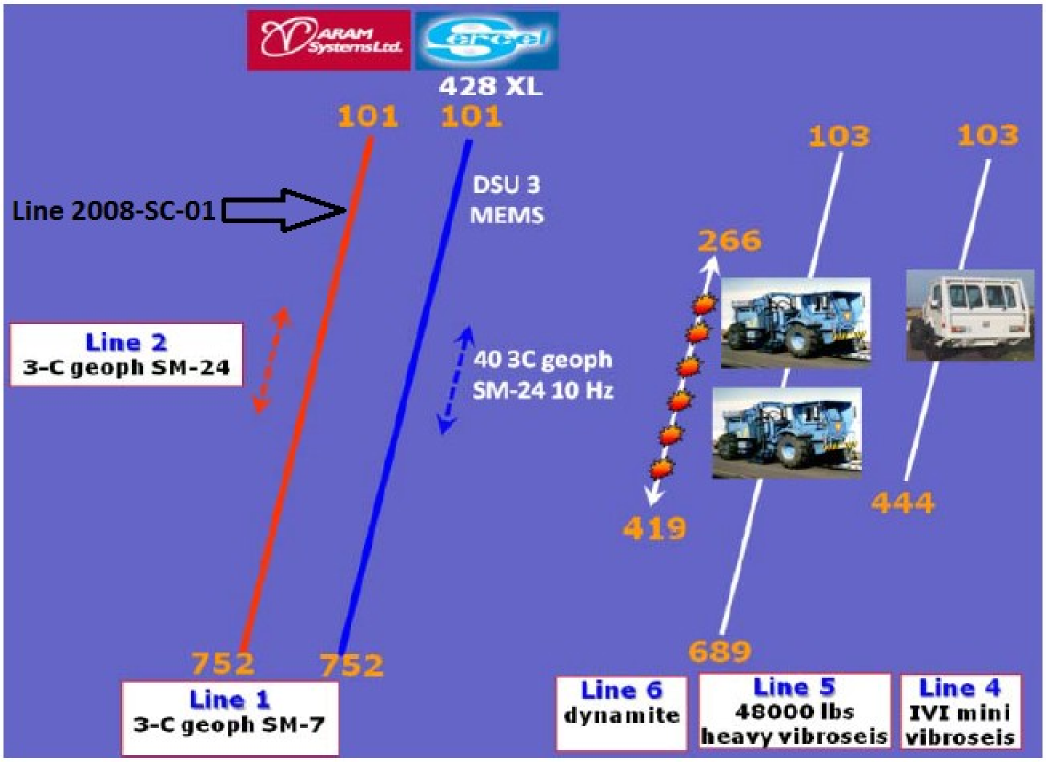

Figure 1.9. Layout of the Spring Coulee survey (Suarez and Stewart, 2008).

Figure 1.10. Right SM7 geophone, left DSU3 MEMS sensor at one station (Bertram et al., 2008).

A three-component Sensor SM24 geophone is installed alongside the other two sensors from station 669 to station 308 (Bertram et al., 2008).

There are three different sources used in this survey. The first source is two Mertz Hemi 48,000 lb vibrators from station 101 to station 689 at every third station. The total shots number is 196. The sweep signal is 4 Hz to 130 Hz over 12 seconds, 4 sweeps per vibroseis shot (Bertram et al., 2008).

EnviroVibe, 18.000 lb, is used in order to obtain data set. Shots are placed at every station 101 to 224, then every third station to 439 and are recorded by SM7 geophones. There are 136 EnviroVibe shots. The sweep signal is 10 Hz to 200 Hz over 12 seconds, 4 sweeps per vibroseis shot (Bertram et al., 2008).

2 kg dynamite charge at 18 m depth is used for this survey from station 266 to station 419 at every third station, 54 dynamite shots are recorded (Bertram et al., 2008).

There are two different systems to record data, Sercel 428XL system and Aries SPMLite recorder system. DSU3 sensors and half of SM24 geophones are recorded by the Sercel 428Xl sytem. On the other hand, SM27 geophones are acquired by the Aries SPMLite recorder system (Bertram et al., 2008).

Line 2008-SC-01 was acquired via two Mertz Hemi vibroseis and were recorded by ARAM (recorder) using SM7 geophones. The line length is 6.5 km. The receiver interval is 10 m, and the shot interval is 30 m. Table 1.1 shows the acqusition parameters for Line 2008-SC-01.

Table 1.1. Line 2008-SC-01 acquisition parameters used in this study.

Line length	6.5 km
Shot interval	30 m
Receiver interval	10 m
Source	Vibroseis
Shot number	196
Receiver number	652
Sample rate	2 ms
Number of channel	592
Record length	6 s
Sweep length	12 s
Minimum offset	10 m
Maximum offset	6490 m

1.4. DATA QUALITY

Several shot gathers of raw data selected from first, middle, and last records are shown in Figure 1.11. The signal-to-noise ratio is good and reflections are visible. Line 2008-SC-01 was analyzed to assess the data quality on selected shot gather 110 (Figure 1.12). Strong reflections are observed on the seismic section with heavy ground rolls and random noise.

Spectral analysis was also conducted for shot gather 110 to examine frequency content of the seismic data (Figure 1.13). The frequency bandwidth is from 12 Hz to 38 Hz for 10 dB amplitude value. Amplitude spectrum shows that data quality is satisfying in terms of frequency.

Optimal parameters used in the processing of Line 2008-SC-01 vertical component seismic data were assigned by testing on selected shot gathers. After determining the parameters, the seismic data were processed with the selected parameters.

1.5. OBJECTIVES

The Spring Coulee 3C-2D data consists of a set of different source and receiver types. The data acquired from the two Mertz Hemi vibroseis and SM7 geophones have good signal-to-noise ratio, however the data contains ground rolls and air blast noises. The data set is selected for reprocessing in order to obtain the better seismic images in the target zone. The main objective is to improve vertical resolution and attain a high quality poststack time migrated section. Various noise suppression techniques are utilized in order to reduce strong noise exhibited on raw shot gathers. The target zone, i.e., the Madison Formation, has been indicated as a potential reservoir in the study area by previous studies (Ostridge et al., 2009). The reprocessing focus is mainly concentrated on the vertical window ranging from 1300 ms to 1400 ms that covers the Madison Formation.

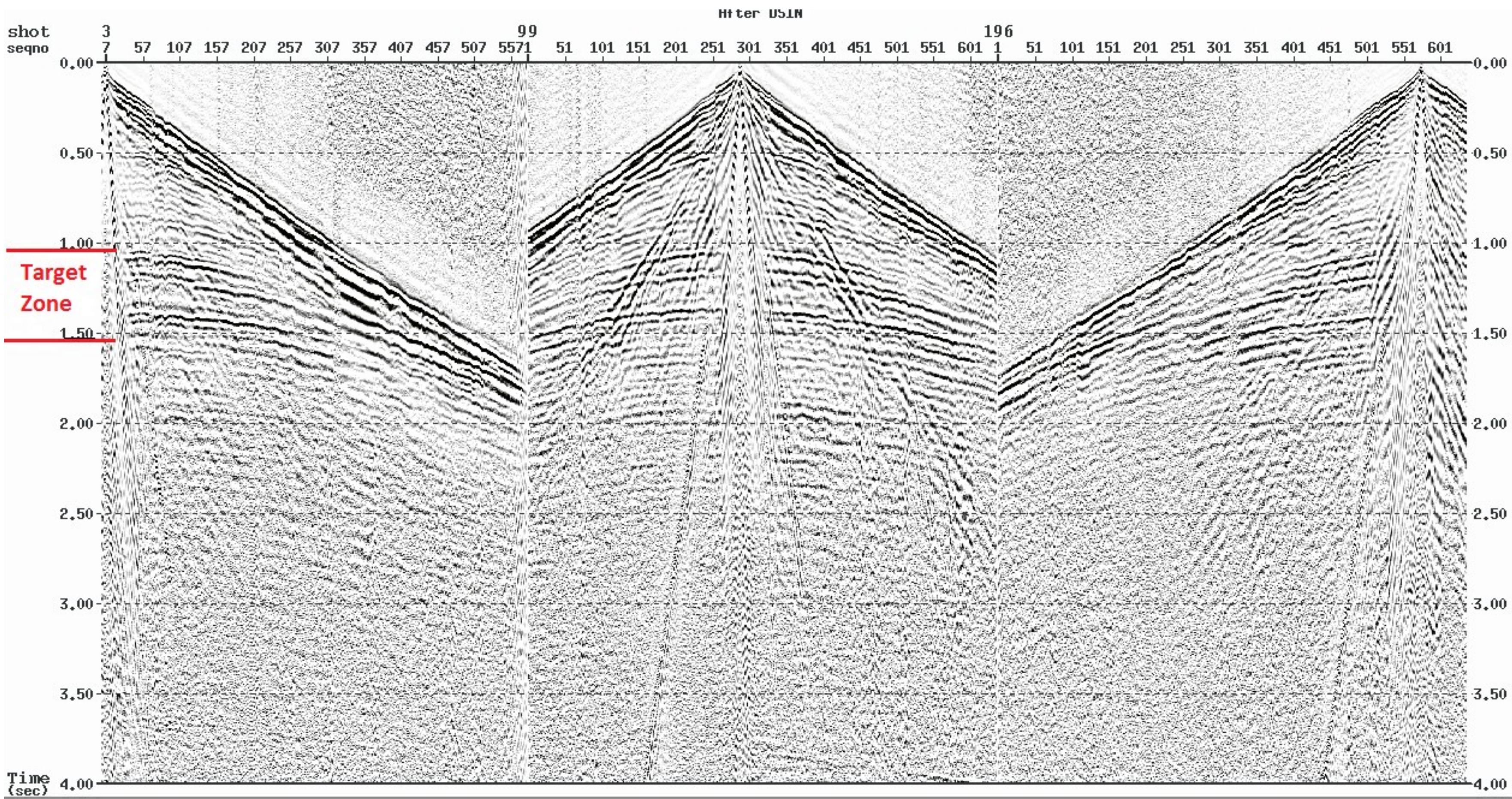

Figure 1.11. Field records of shots 3, 99, and 196 with AGC applied.

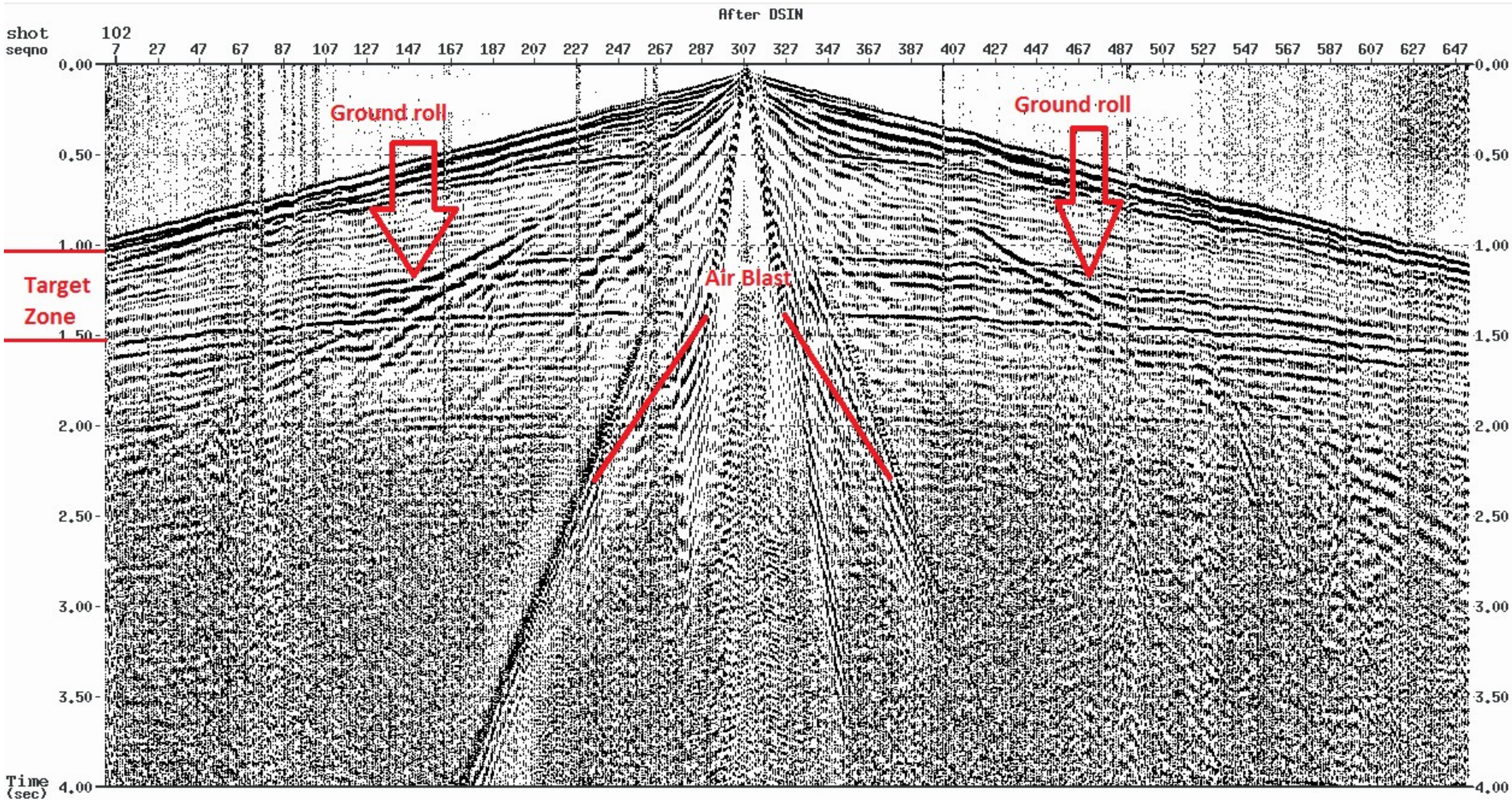

Figure 1.12. Shot gather 110 showing with the air blast noise and ground roll.

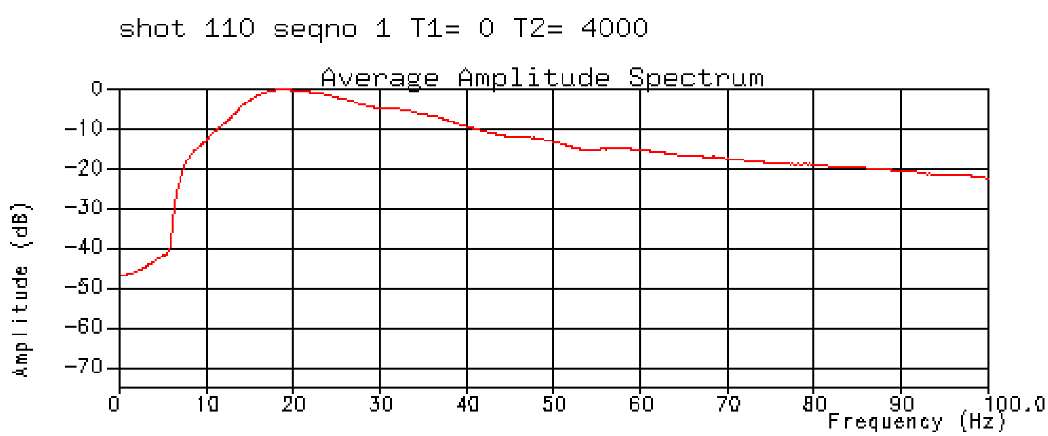

Figure 1.13. Amplitude spectrum of shot gather 110.

2. METHODOLOGY

In order to process the Spring Coulee Line 2008-SC-01 seismic data, the processing software of Echos by Paradigm (version 17) was used. Several shots of the data were selected from first, middle, and last records to decide which parameter is suitable for the seismic data. Then, these paramaters were applied to all datasets.

The processing flow was created by testing parameters, methods, and algorithms such as deconvolution, static correction, and migration (Figure 2.1). After deconvolution, stack was applied to analyze the effect of the processing steps. Although this data contains some noises such as air blasts and ground rolls, reflections are clear and seismic data quality is good. The main target on the data is between 13000 ms and 1400 ms. The areas between 1400 ms and 2500 ms contain reflections. The areas below 2500 ms are not considered because seismic quality reduced, and there was not any reflection there. In this study, the results from applying processing steps are presented in details.

2.1. DATA IMPORT AND GEOMETRY

Data import and geometry are in the pre-processing part, which they lay foundation for the following processing steps such as static corrections and CMP sorting.

Seismic data are recorded in a multiplexed mode. The data first are demultiplexed, which is the mathematical operation of transposing a big matrix. This matrix is arranged seismic traces acquired at different offsets with a common shot point. In this process, the data are converted to a specific format that is used during the seismic processing. Seismic data are stored in a specific format determined by companies (Yilmaz, 2001).

The most popular formats are SEG-D and SEG-Y. The seismic data used in this study were recorded as the SEG-D format. Then, it was converted to the SEG-Y format (Drijkoningen and Verschuur, 2003).

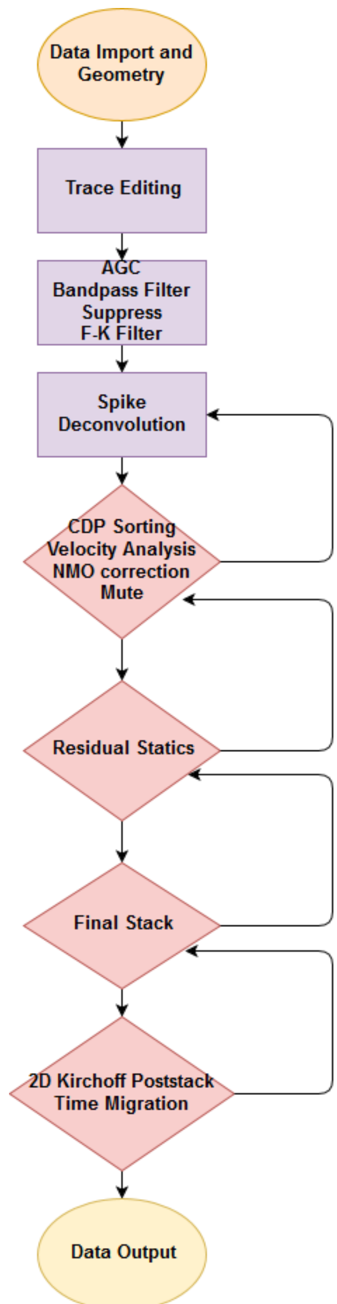

Figure 2.1. Line 2008-SC-01 processing flow chart.

Seismic data are sorted into the CMP gather so that the geometry of the acquisition layout, which contains the source and receiver locations, group spacing, stations and others, must be defined on the seismic processing software (Lee et al., 1999). In this study, when the data were imported to the processing software, elevations of sources and receivers were not correct. In order to fix this complication, elevations were restored manually. Figure 2.2 and Figure 2.3 show the shot and receiver locations and elevations used in this survey, respectively.

The offset plot is used to verify the offset geometry relationships. The offset should be sustained by the distance from the shot to receiver. Figure 2.4 represents the offset plot for selected shot gathers.

Line 2008-SC-01 consists of 652 channels. Source interval is 30 m and receiver interval is 10 m. The obtained fold number is 98.

2.2. TRACE EDITING

Trace editing, which is a pre-processing step, is needed to handle noisy seismic records (Pokhriyal et al., 1992). During seismic data acquisitions, bad shots or bad traces occur, and they lead to degradation of the seismic data. For instance, during the processing of a shot gather, a bad trace or bad dead shots will affect the result. Thus, all bad shots and/or noisy traces are edited or omitted at an early step of processing for further the processing steps.

Dead shots or missing traces cause the artifacts at the edges of the dead data, so they are omitted or filled with zeros before applying noise attenuation. Therefore, observer logs must be analyzed to check dead shots or bad traces.

Before the integration of leading-edge technology in seismic acquisition and seismic processing, the manual edition of seismic traces were applied. A great amount of time were spent on manual editing because the volume of seismic data were large. In recent years, automatic trace editing is common.

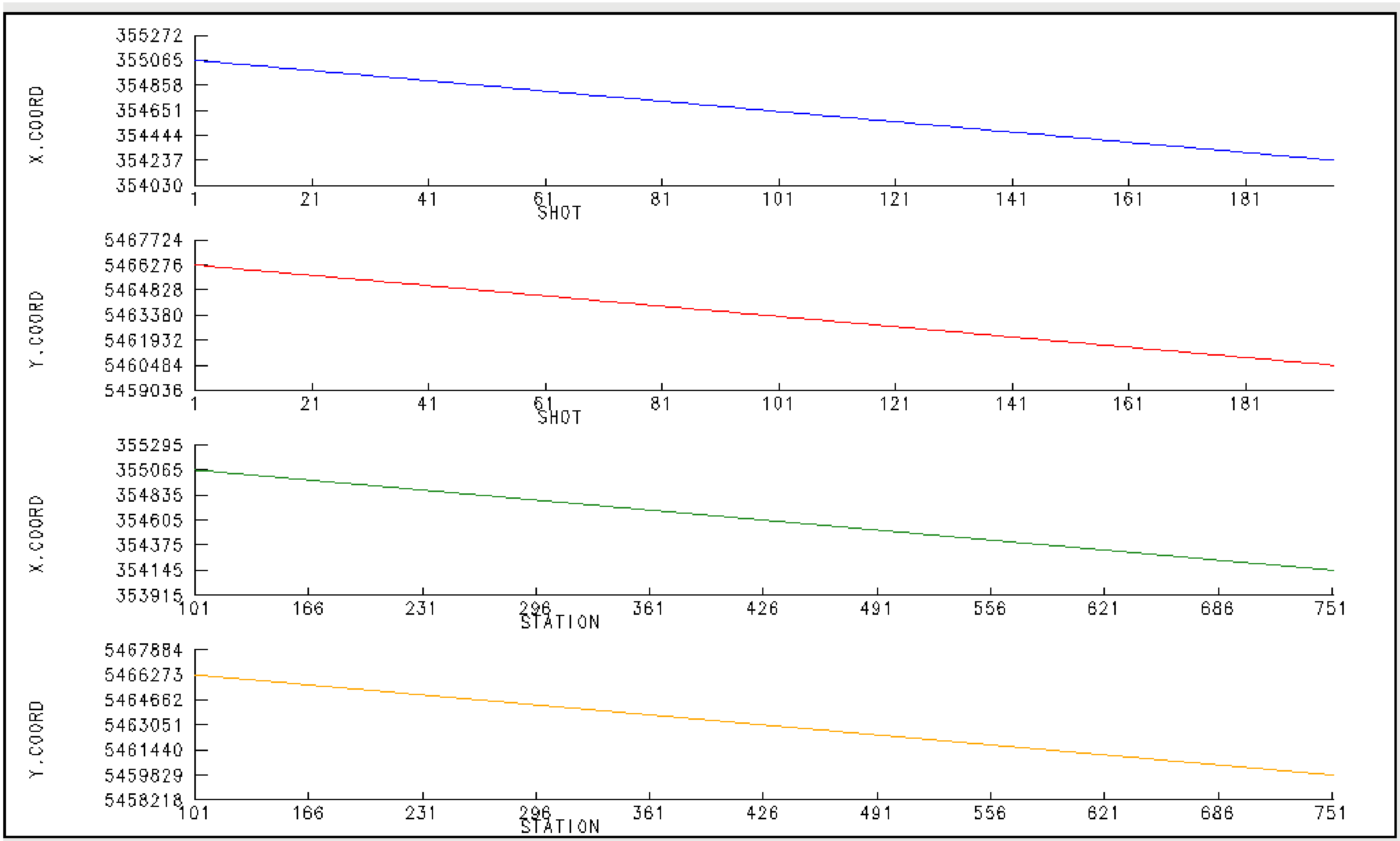

Figure 2.2. Diagram showing locations of shot and receiver stations. X axis represents the number of shots and stations while Y axis indicates the coordinates.

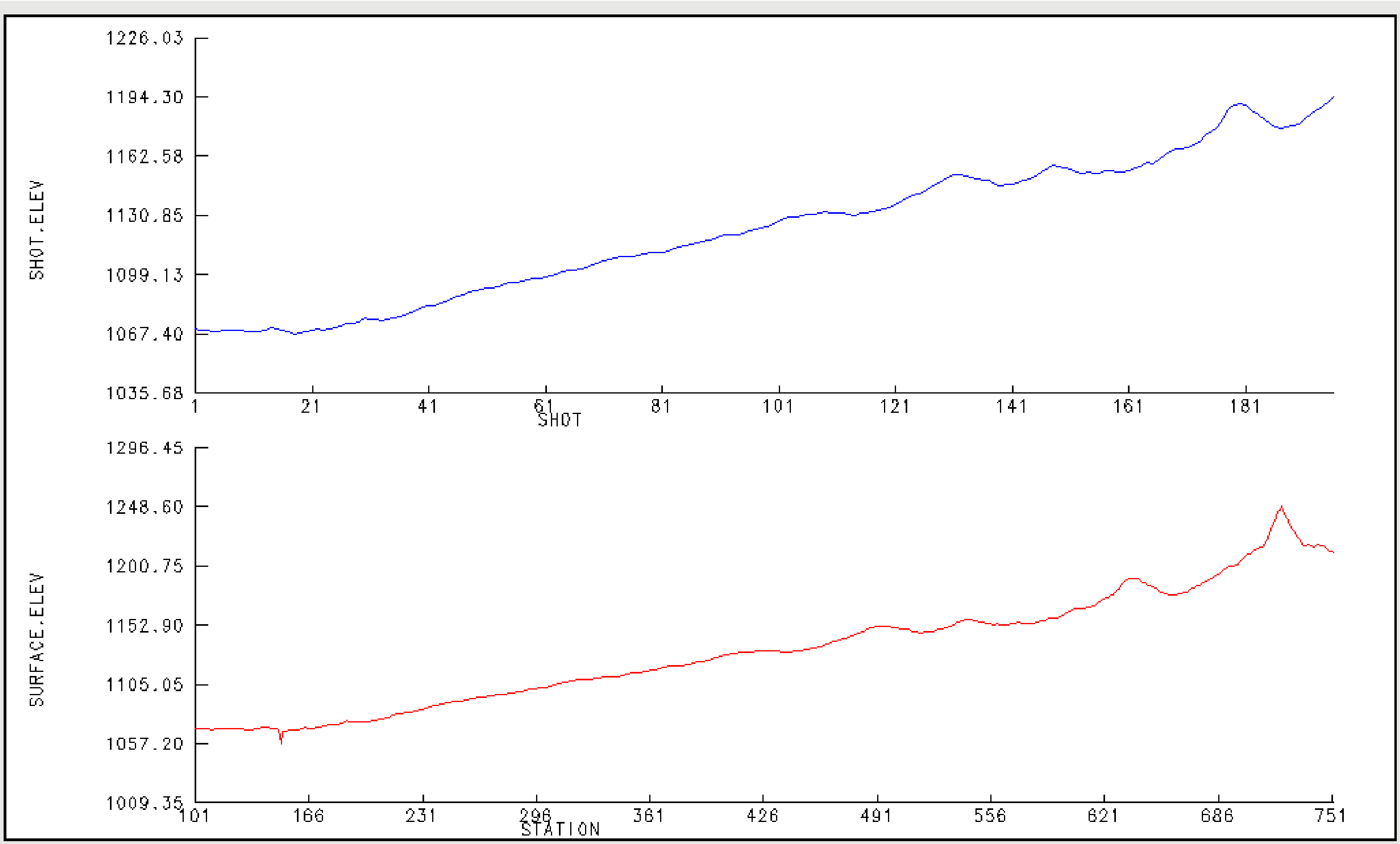

Figure 2.3. Illustration of shot and receiver elevations. X axis represents the shot and receiver station numbers, and Y axis indicates the elevations in meter.

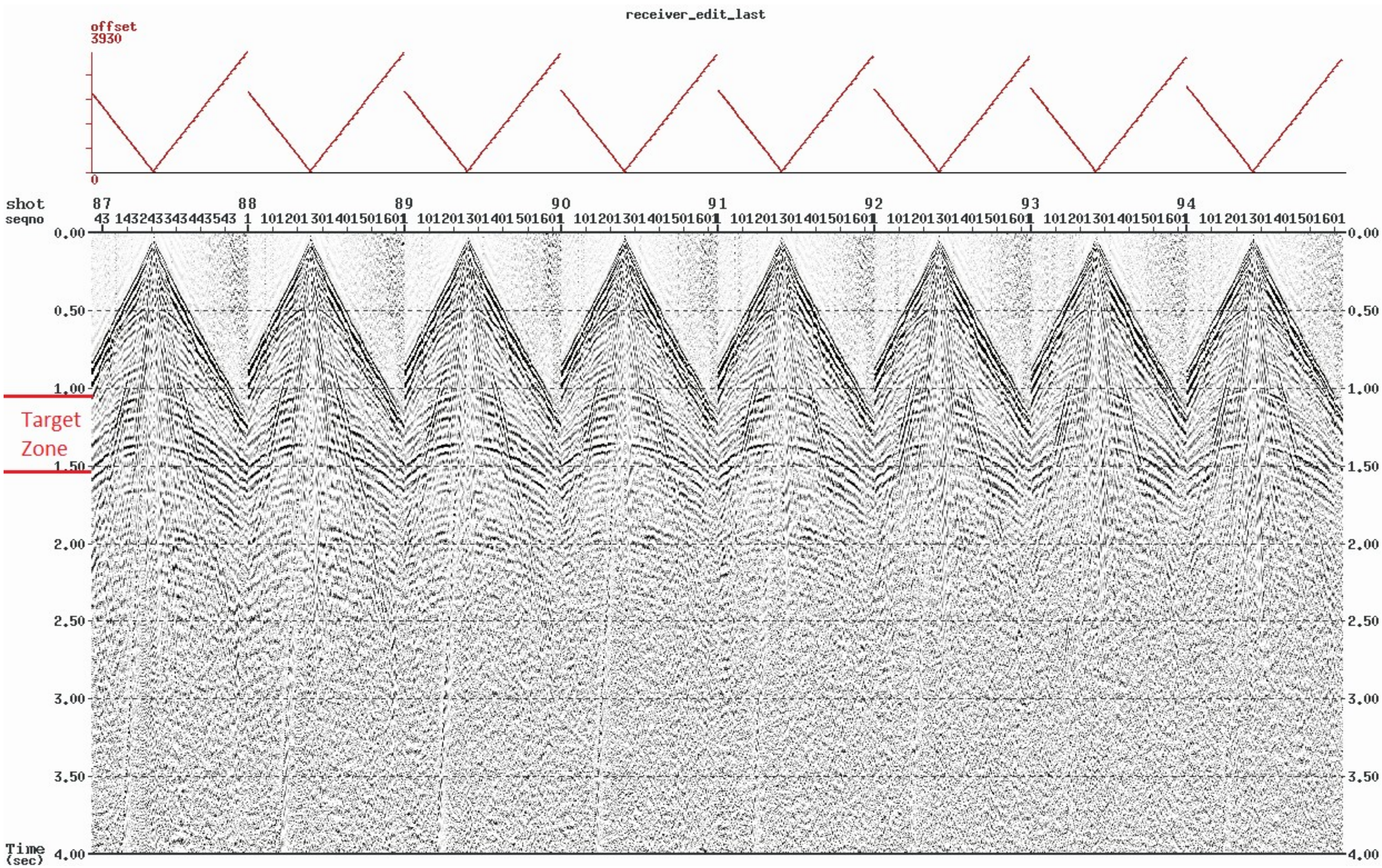

Figure 2.4. Selected shot gathers 87-94 showing with offset.

All shot gathers contain noises. Some noises can be tolerated in the trace editing section because they can be omitted in the noise attenuation stage to avoid data lost. On the other hand, some noise effects are so strong on the data, and they influence the quality of further processing steps. In this study, the first and second shot include strong noise, affect the signal-to-noise ratio, and also demolish the reflections. Therefore, the first shot and the second shot were omitted during the trace editing stage. Although shot gather 3 includes some noise, they can be suppressed during the noise suppressing because reflections are clear. Therefore, shot gather 3 did not omitted. Figure 2.5 shows shot gather 2 and shot gather 3.

2.3. STATIC CORRECTIONS

Static corrections are applied to seismic data to balance the influence of variations in weathering velocity and thickness, and elevation (Sheriff, 2002). Therefore, for land data, static corrections are an essential processing step because they affect the qualities of ensuing processing steps and resolution of the migration result. In order to conduct static corrections, correcting near-surface and elevation variations play a key role (Deere, 2009). Incorrect static results in low quality resolution, both spatial and temporal, and it could be an obstacle during the interpretation stage (Zhu et al., 2014).

Non-planar reflectors, near surface low velocity zones, and rugged surface acquisition are reasons to apply static corrections. They are based upon short wavelengths (small shift in time) and long wavelengths (larger time shifts). Static corrections are used to solve the effect of long wavelengths, while residual static methods are effective to remove short wavelengths effect. Residual statics methods are discussed later in this study (Li et al., 2006).

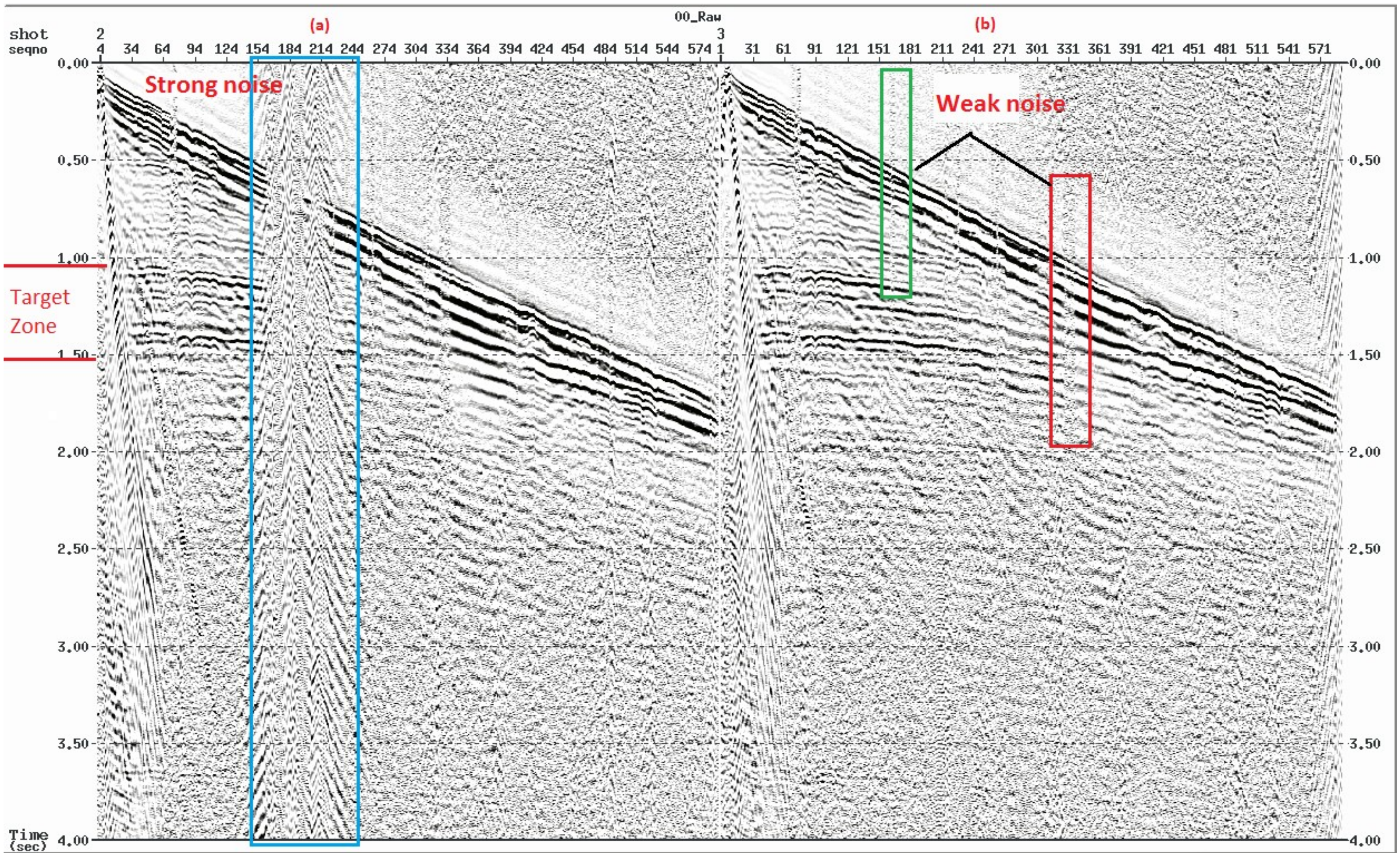

Figure 2.5. a) Omitted shot gather 2 due to strong noise. b) Shot gather 3. Noises are not strong, so it is not omitted.

Static correction methods include field statics, also known as elevation statics or datum statics, refraction statics, and residual static corrections. Elevation statics include the weathering corrections and the elevation corrections for removing effect of near-surface layers and source and receiver elevations (Al Mukhtar and Aswad, 2016).

In this study, elevation static corrections were applied to the data. Computed statics for receiver and shot stations are shown in Figure 2.6 and Figure 2.7, respectively.

2.4. NOISE ATTENUATION

Figure 2.9 illustrates selected shot gathers before processing. The geometrical spreading of the wavefront causes seismic wave amplitude decay. Therefore, automatic gain control (AGC) was applied to the seismic data to improve the amplitude of the seismic data (Figure 2.10).

Seismic data frequently contains seismic noises such as ground rolls, swell noise, and air blast. The purposes of the noise attenuation are to suppress the seismic noise and improve the signal-to-noise ratio. The first step in noise attenuation is to analyze the seismic data in order to determine the sources of the noise and the noise characteristics. The seismic noise is divided into two categories, which are coherent noise and incoherent noise. The other classifying noise type is whether noise is repeatable or not.

Coherent noise contains surface waves, refractions, and multiple reflections. Coherent noise except multiples travel horizontally and, all except vehicular noise such as cars and trucks noise are repeatable on shots. Thus, coherent noise is categorized by energy that travels horizontally or reaches the spread more or less vertically (Talagapu, 2004).

Incoherent noise is also known as random noise, which indicates non predictability and certain statistical properties. Small scale faulting and near surface irregularities generate incoherent noise. Also, wind blowing, a person walking near a receiver, distant earthquakes, and movement of the roots of trees may create random noise (Talagapu, 2004). There are several methods to eliminate coherent noise or random noise (Table 2.1).

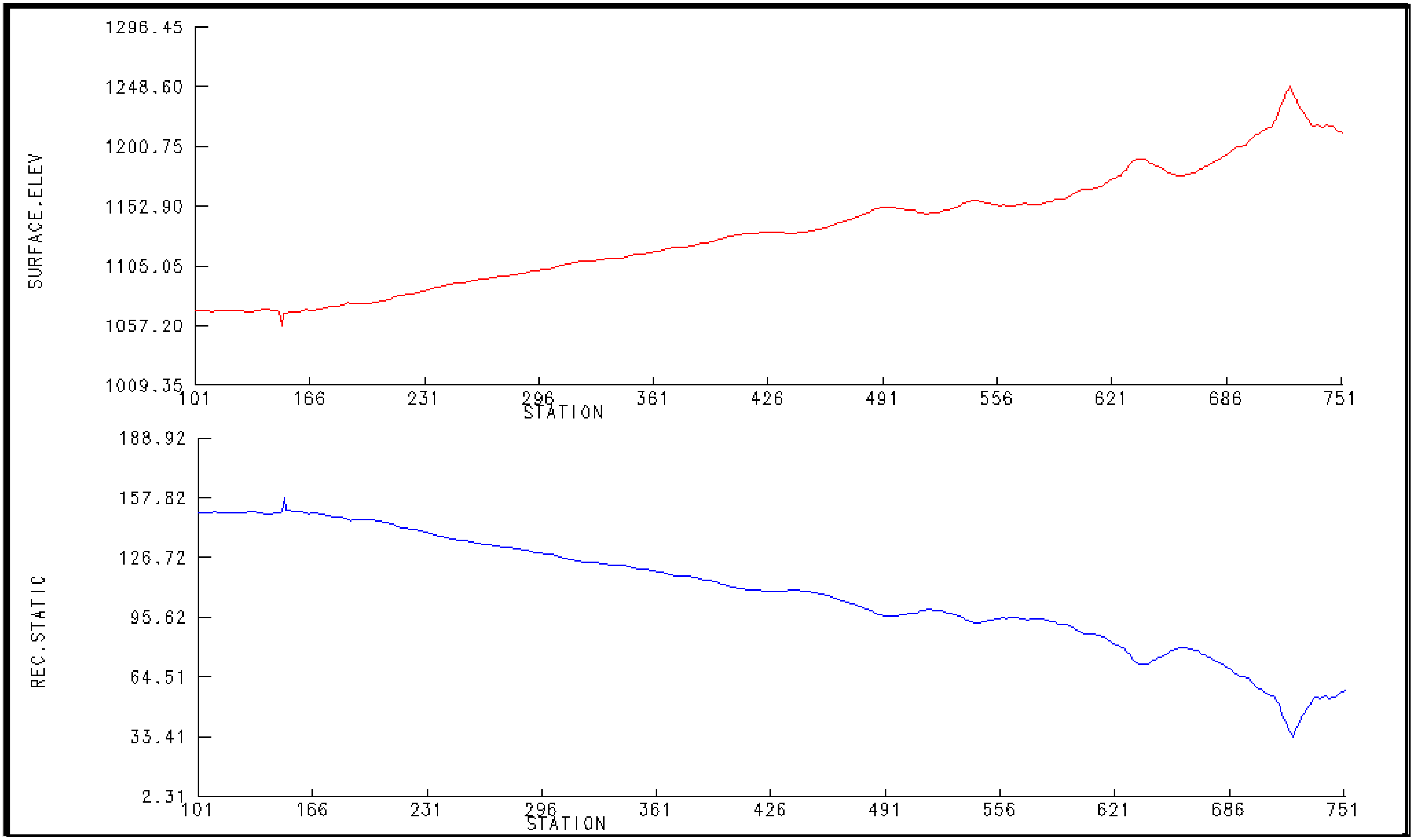

Figure 2.6. Static correction for receivers.

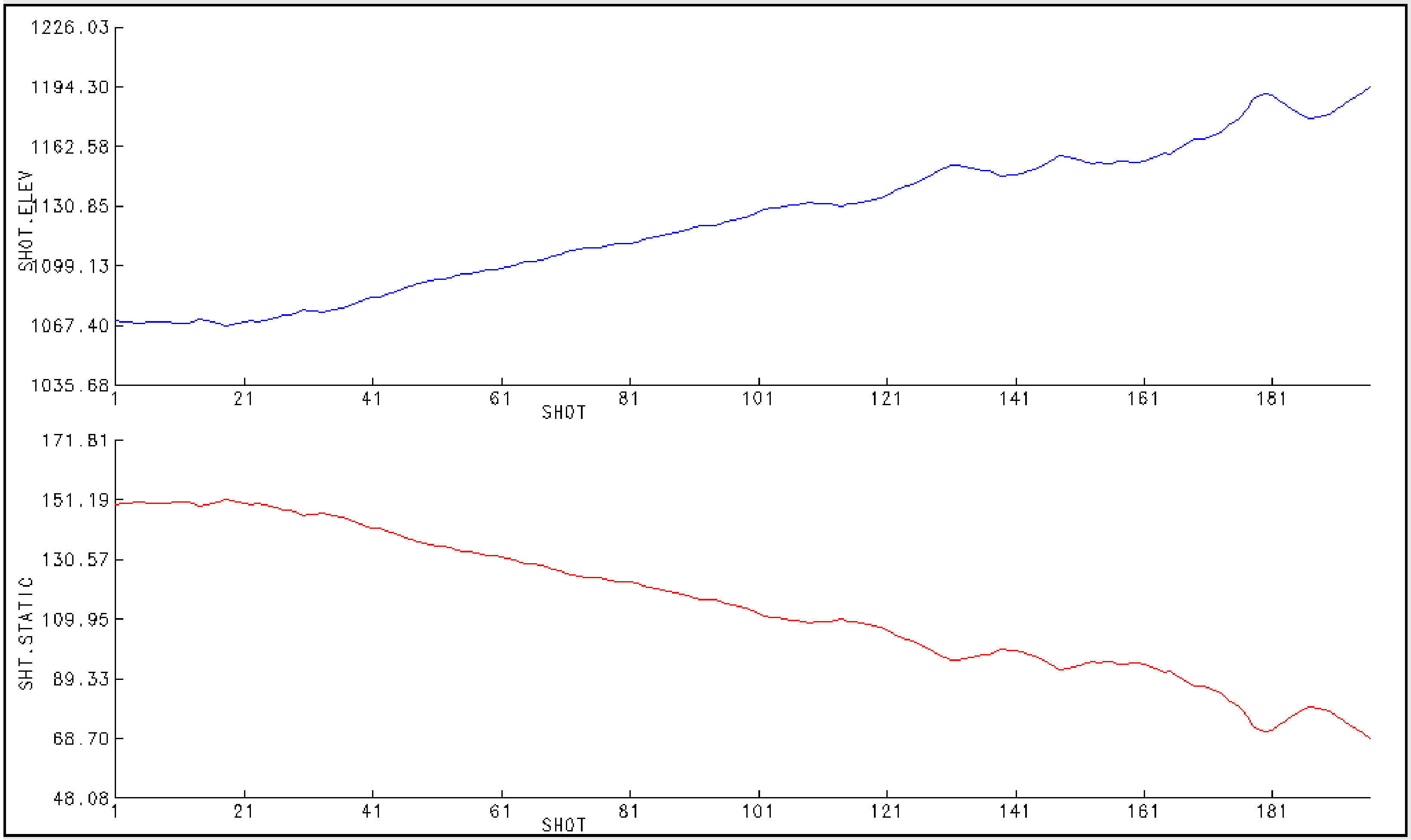

Figure 2.7. Static correction for shot locations.

Table 2.1. The methods applied to seismic data in order to suppress random and coherent noise.

Random	**Coherent**
Band pass filtering	Band pass filtering
Notch filtering	Velocity filtering i.e. F-K filtering
K-filtering	Muting
F-K filtering	Coherency filtering
Stacking	
Editing	
Coherency filtering	
F-X filtering	

The energy source on land generates an airwave, which is known as the air blast. Velocity of the air blast is approximately 350 m/sec. The speed could be changed due to temperature and humidity (Talagapu, 2004).

Seismic sources compose ground rolls due to the nature and position of the source, and near surface environment, and ground rolls generally occur on the land seismic data (Deighan and Watts, 1997). Ground rolls are defined with low frequency, high amplitude, and low velocity. Ground rolls cause some factors such as reducing the signal-to-noise ratio, incorrect velocity analyzing, and lowering quality of stacking and migrating steps (Chiu et al., 2008). A seismic trace includes high frequency ambient noise and low frequency noise such as ground rolls. The seismic energy bandwidth is between 10 Hz to 70 Hz. In general, dominant frequency is approximately 30 Hz. In order to suppress these noises, several frequency filtering can be applied such as high pass (low cut), or low pass (high cut) band pass, and band reject. Band pass filtering, which is a combination of low pass and high pass filtering is efficient method to suppress low frequency and high frequency noise (Yilmaz, 2001). Therefore, in order to suppress the ground rolls, band-pass filter was applied to the data, and acquired results are shown in Figure 2.11. After applying the band pass filtering, the low frequency and high frequency noise were reduced significantly.

The suppress module performs time-variant band-limited noise suppression, such as ground roll or swell noise. Data are decomposed into good and bad signal bands and time-variant noise suppression is then performed by thresholding the noise envelope with the signal envelope. After band pass filtering, the data still contain ground rolls and air blast. Thus, to remove these noises, the suppress module was applied to the seismic data and the result shows removed noise (Figure 2.12).

The F-K filtering is also known as dip filtering. In general, coherent linear noise, guided waves, and ground rolls obscure reflections, but they can be distinguished in the F-K spectrum (Yilmaz, 2001). Figure 2.8 shows the F-K spectrum of seismic events and typical noises. In order to eliminate linear and random noise of the seismic data, the F-K filtering is commonly applied (Chen et al., 2015).

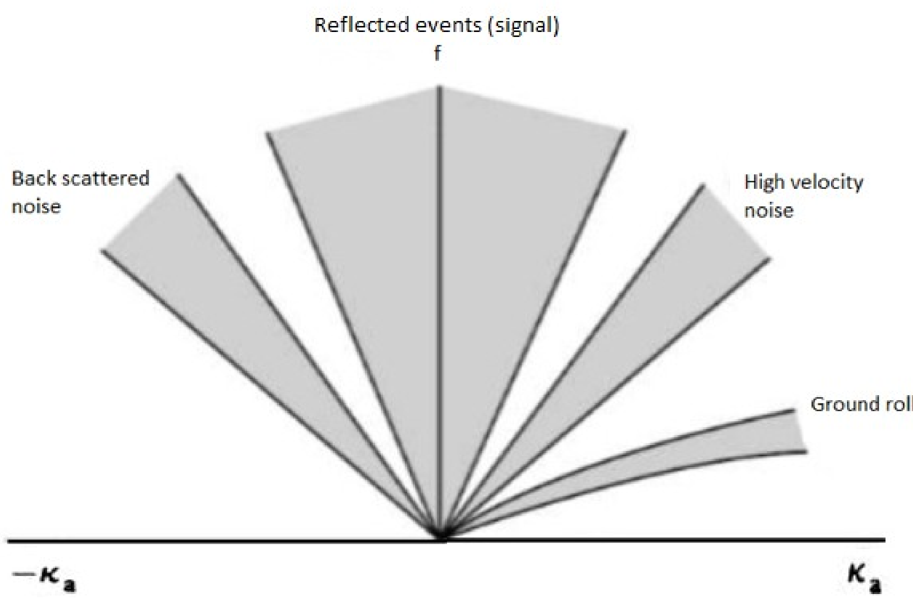

Figure 2.8. F-K spectrum of the seismic events and noises.

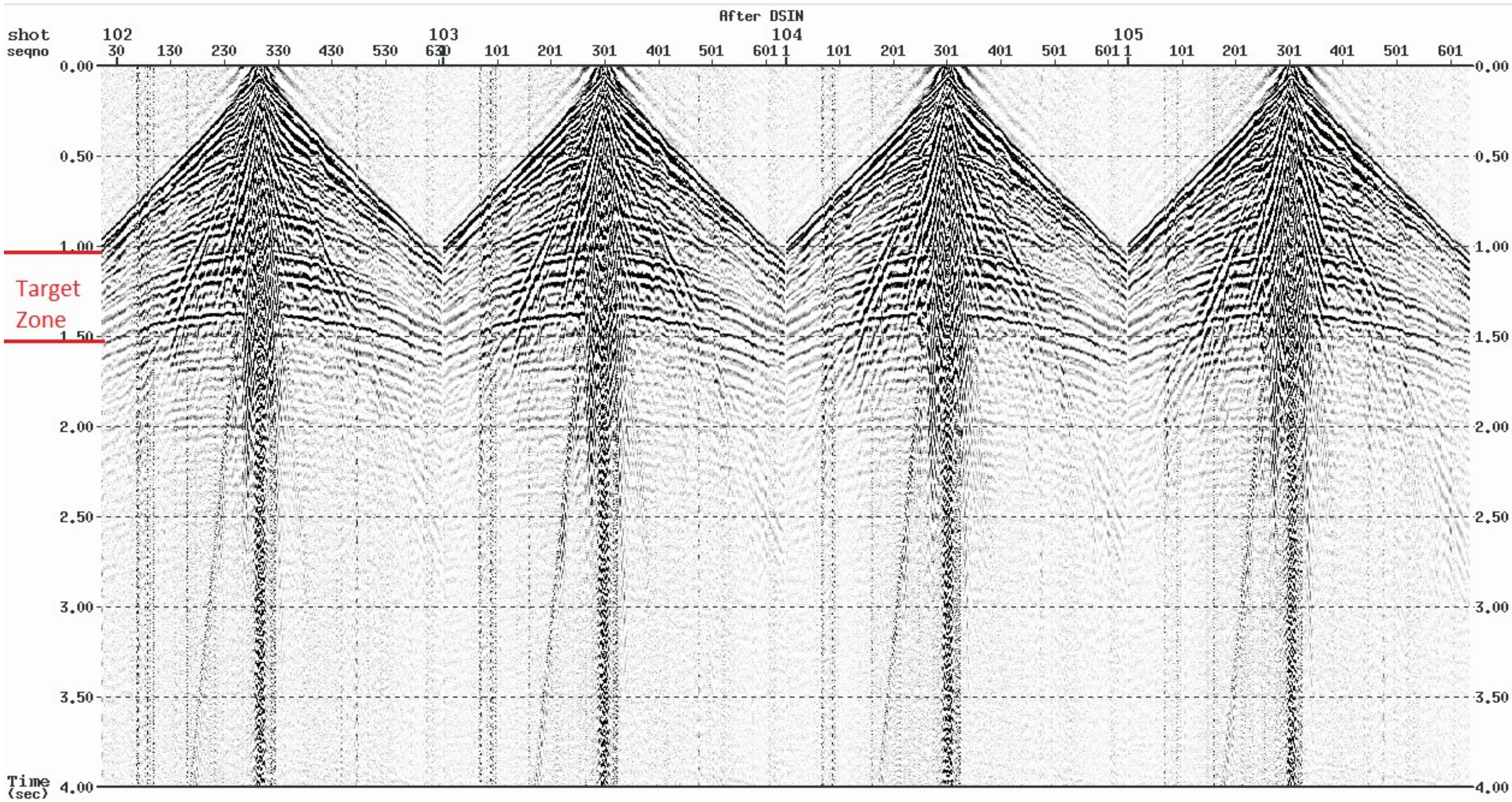

Figure 2.9. Shot gathers from 102 to 105 before processing.

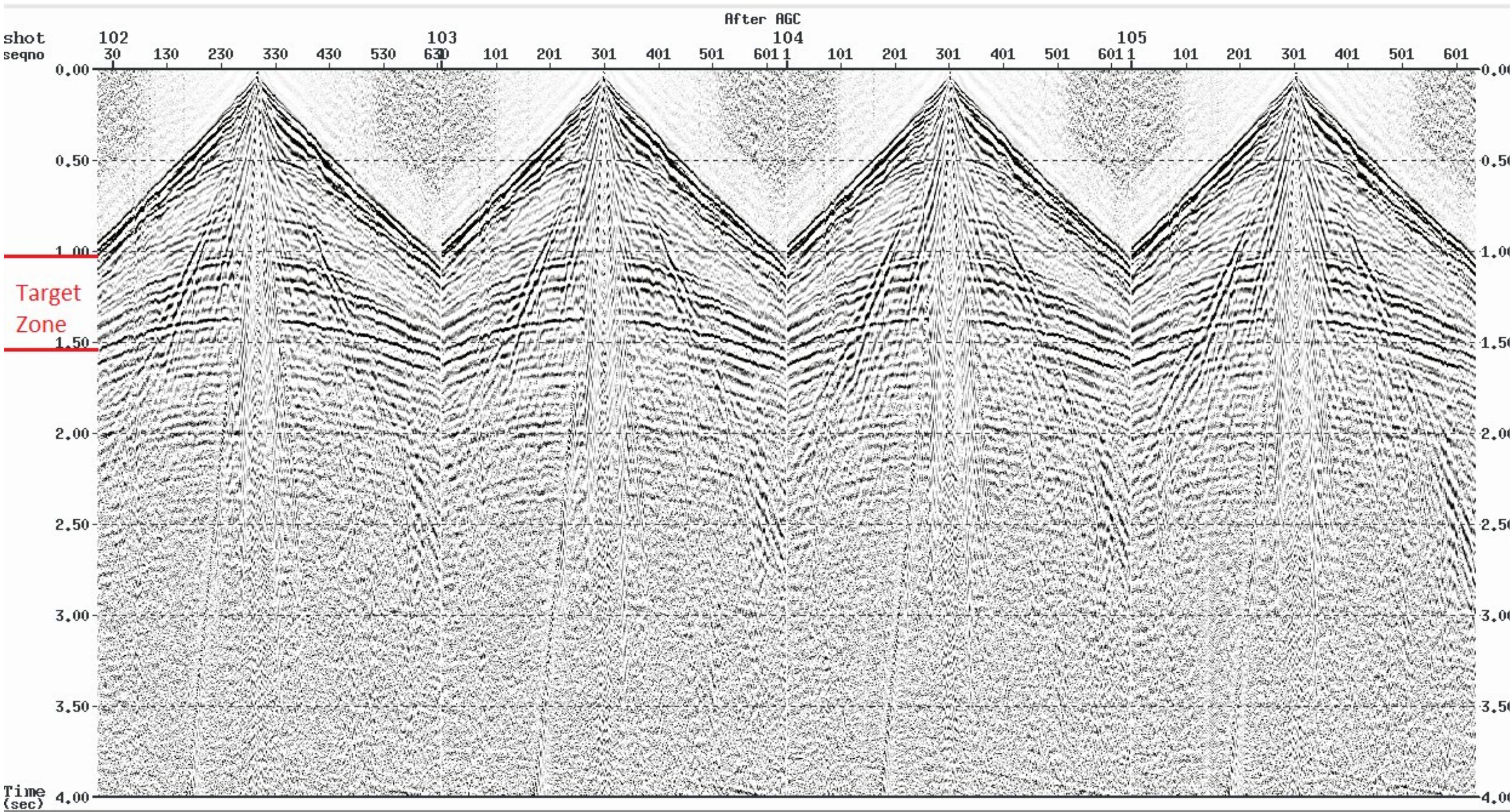

Figure 2.10. Shot gathers from 102 to 105 with AGC applied.

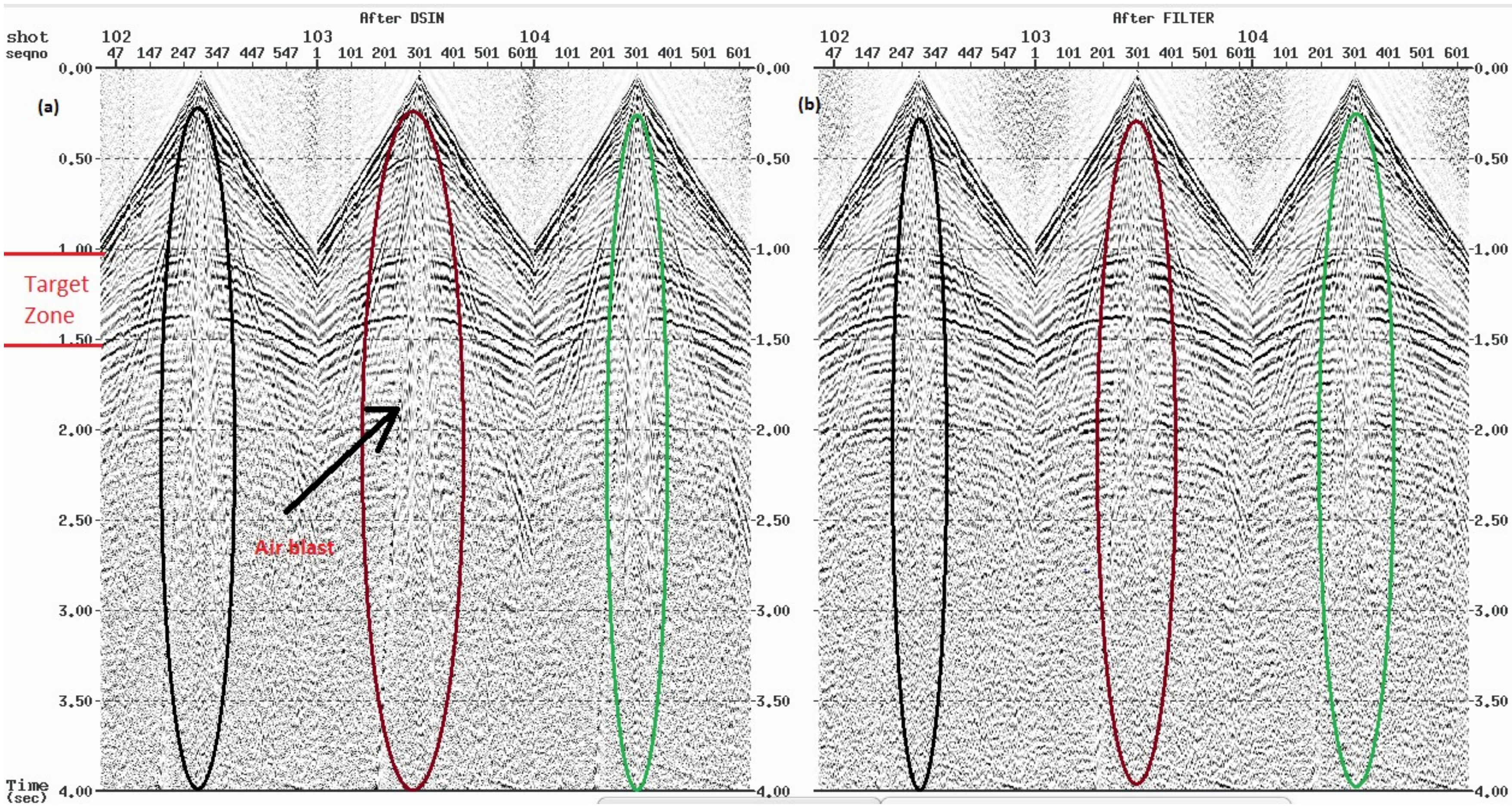

Figure 2.11. Shot gathers from 102 to 104. a) Before band pass filtering. b) After band pass filtering from 10 Hz to 75 Hz. Lower and higher slopes are 32 dB/octave and 34 dB/octave, respectively. Band-pass filtering applied has improved data. The air blast was partially suppressed.

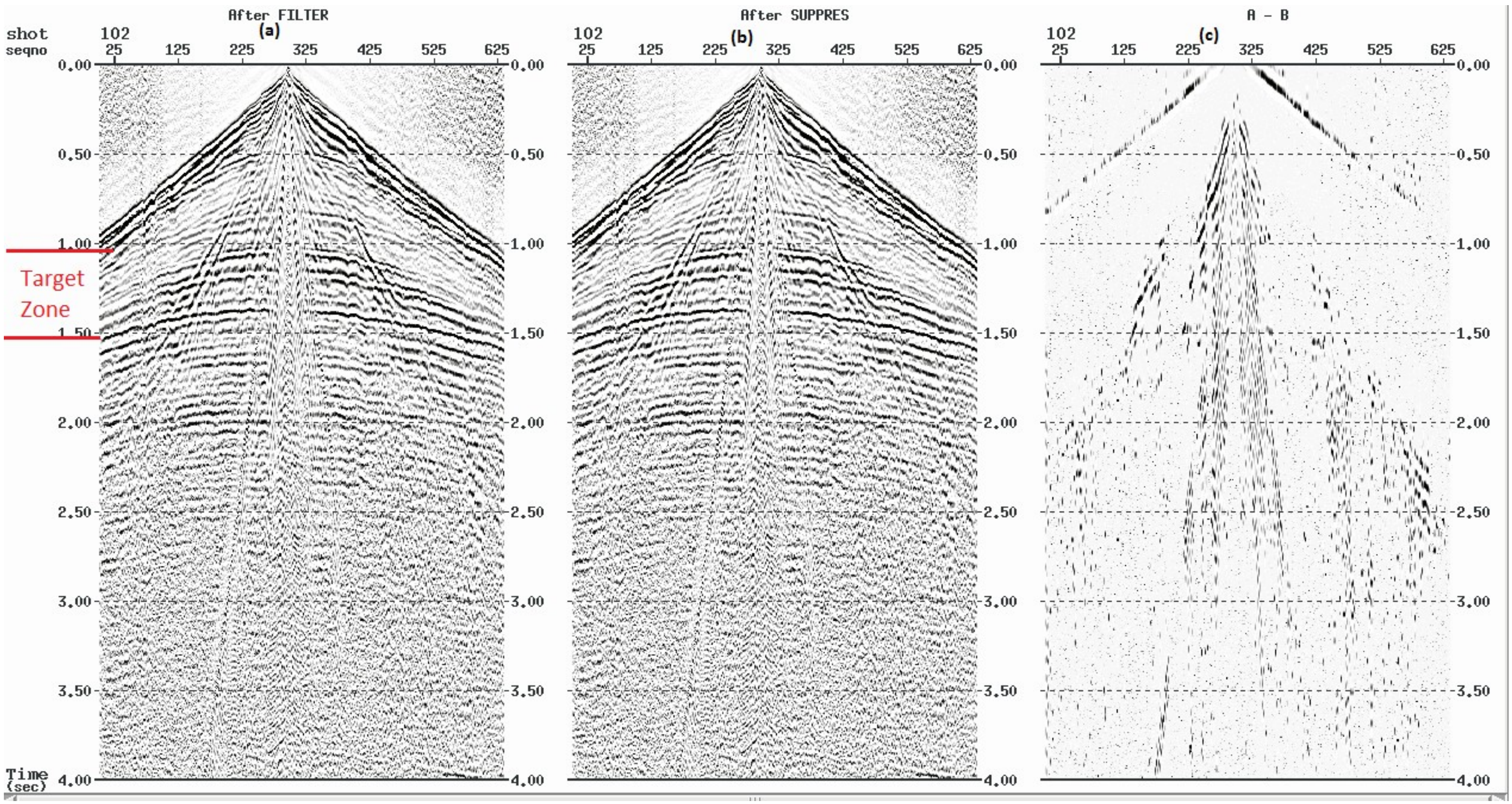

Figure 2.12. Shot gathers from 102 to 104. a) Shot gather 102 before the suppress module applied. b) Same shot gather after the suppress module applied. c) The difference between before and after the supress module applied.

In many situations, band pass filtering is not enough to eliminate a certain type of noise. In this study, although band pass filtering and a suppressing module were applied, the data still contained ground rolls which caused the quality of reflections placed in the target area, and decreased the signal-to-noise ratio. Therefore, the F-K filtering was used two times to the seismic data in order to suppress ground rolls (Figures 2.14 and 2.15). First F-K filtering was applied on the positive wave number, and second was applied on the negative wavenumber.

The important point is to avoid spatial aliasing while applying the F-K filtering. Spatial aliasing causes dispersive noise that reduces the quality of seismic data. Seismic data with no spatial aliasing problems are typically clear of steep dipping events that are associated with low velocity. Figure 2.13 represents an aliasing problem.

Ground rolls in data are associated with velocity around 1200 m/s, which is too high to be aliased for group interval. However, air blasts have a low velocity and are severely spatially aliased. In order to prevent the aliasing problem, further noise suppression processes are required. For instance, the suppress module was utilized to reduce air blast spatial aliasing in particular with specific parameters. Figures 2.16 and 2.17 show that spatial aliasing is not observed on the F-K spectrum.

The seismic data was influenced by seismic noise, as mentioned previously in the data quality section. During the noise attenuation stage, several parameters were checked to suppress the seismic noise. The shot 102 was selected to check these parameters, and then the selected parameters were applied to the seismic data. The obtained result suggested that air blast and ground rolls were suppressed efficiently, reflections were stronger, and the signal-to-noise ratio was improved for further processing steps. The final results applying several noise attenuation methods are shown in Figure 2.18.

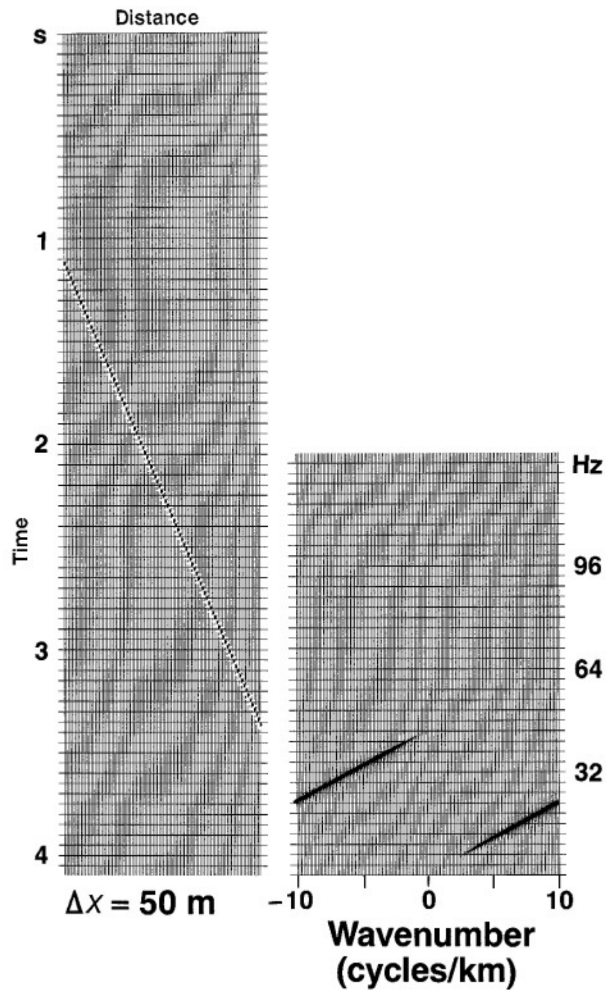

Figure 2.13. F-K spectrum of the seismic event and noises (Yilmaz, 2001).

2.5. DECONVOLUTION

Deconvolution is a crucial processing step in seismic exploration. It is an inverse process of convolution (Velis et al., 2006). In order to understand deconvolution, the earth impulse response is essential. The earth consists of rock layers that have different lithology and physical properties. The densities and velocities characterize the rock layers. They compose the acoustic impedance, which leads to seismic reflections recorded along a surface profile. In this way, to obtain the seismogram, convolution of the seismic wavelet is used, containing waveshape pattern, recording filter, surface reflections, and geophone response. The impulse response occurrs, if the wavelet is just a spike, and this impulse response includes reflections and all possible multiples. Enhancing the temporal resolution of seismic data by the wavelet is a result of deconvolution (Yilmaz, 2001).

Norbert Wiener developed a mathematical algorithm that separates radar signals from noise during the World War 2. This is also known as smoothing or Wiener filtering. The reversing of this filtering is a processing of a deconvolution, and then this filtering was integrated into processing reflection seismic data. Therefore, all types of deconvolution such as predictive deconvolution and spiking deconvolution are based on the Wiener filter theory (Leinbach, 1995).

Spiking deconvolution is used so as to compress the effective source wavelet included in the seismic traces in order to enhance temporal resolution (Yao et al., 1999). In this study, spiking deconvolution was applied to obtain sharper seismic events and have a frequency bandwidth filter (Figure 2.19).

Predictive deconvolution is a single trace operator (Zhou, 2014). The autocorrelation of the source wavelet, gap, and operator length are required in order to use predictive deconvolution. These parameters are applied to the data in the time domain (Broadhead et al., 2007). Predictive deconvolution is generally used to remove multiple reflections (Ulrych and Matsuoka, 1991). Also, it can be applied to alter the spectrum of the input data to enhance resolution. Land seismic vibrator data can generate multiple reflections. In this study, the source was vibroseis, but multiple reflections were not observed on the data.

The spectral analysis was introduced before and after the spiking deconvolution to analyze recovery in the frequency bandwidth (Figures 2.20 and 2.21). The analysis of the amplitude spectrum represents that frequency bandwidth was expanded.The frequency bandwidth was from 10 Hz to 38 Hz before the spiking deconvolution, while it was enhanced from 8 Hz to 92 Hz for 10 dB amplitude value after the spiking deconvolution.

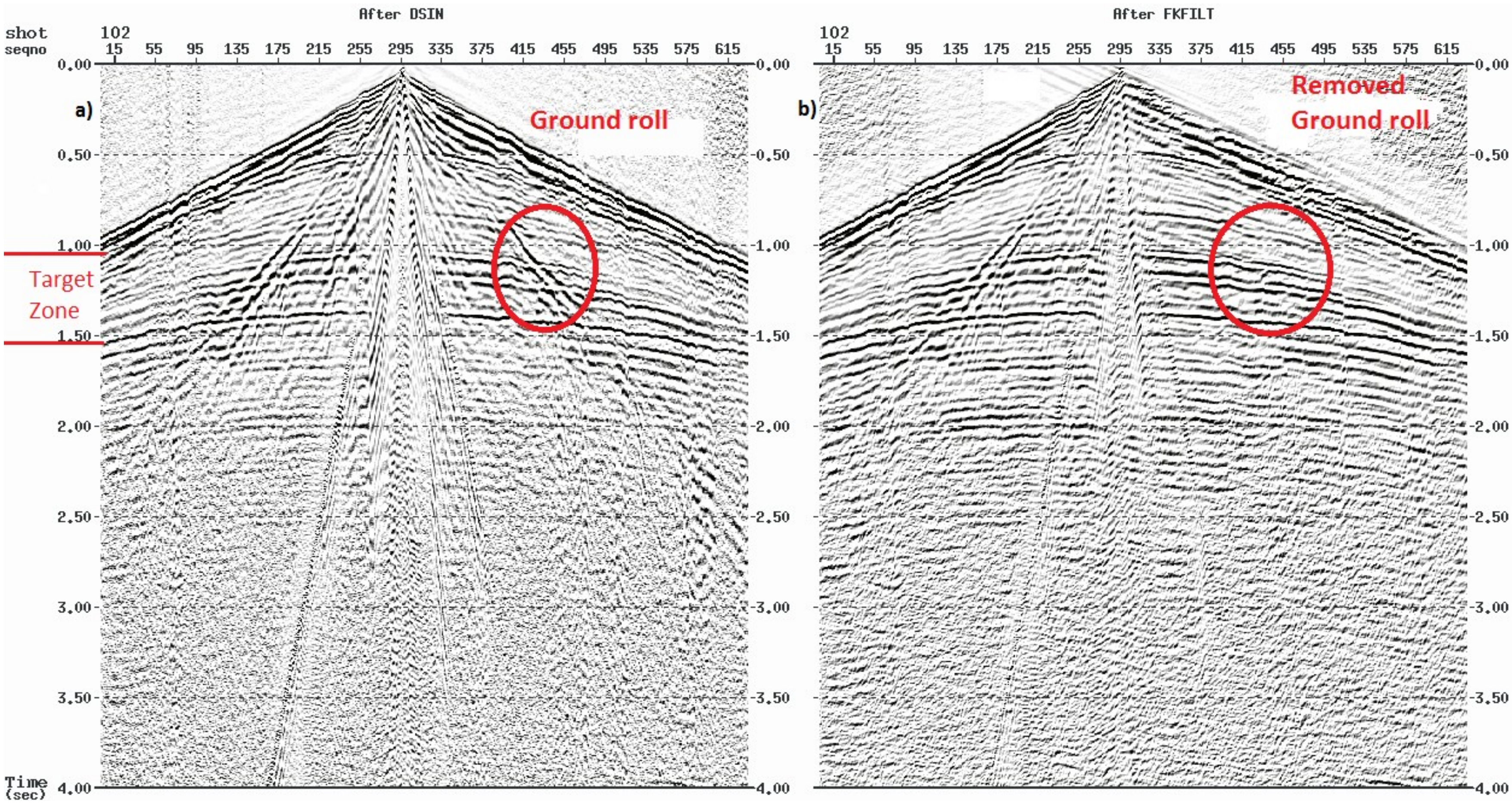

Figure 2.14. Shot gather 102. a) Before F-K filtering. b) After F-K filtering with the positive wave number. Ground rolls were suppresed clearly.

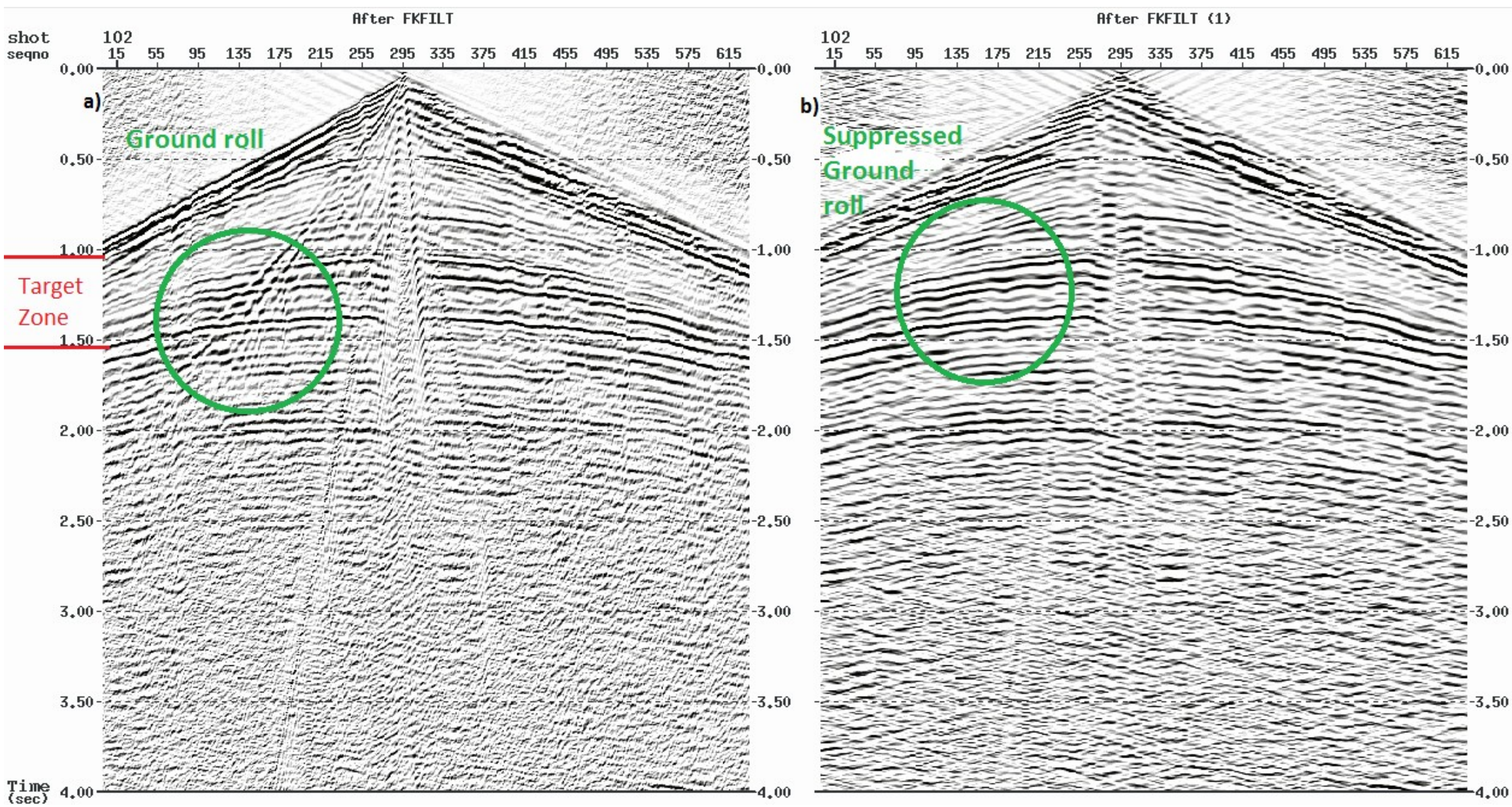

Figure 2.15. Shot gather 102. a) After F-K filtering. b) After F-K filtering with the negative wave number. Ground rolls were suppressed notably.

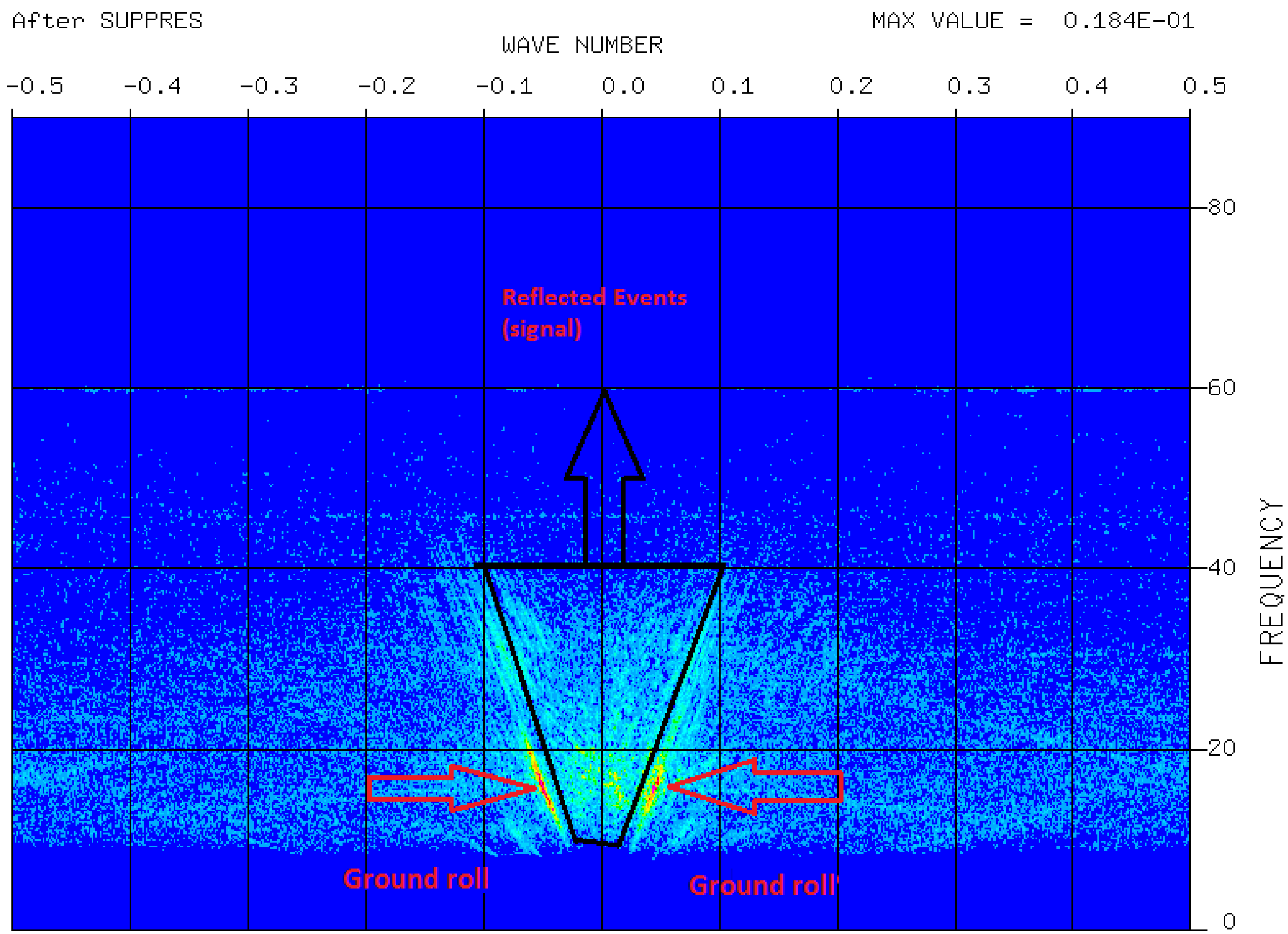

Figure 2.16. F-K spectrum before the F-K filtering. The data contain ground rolls.

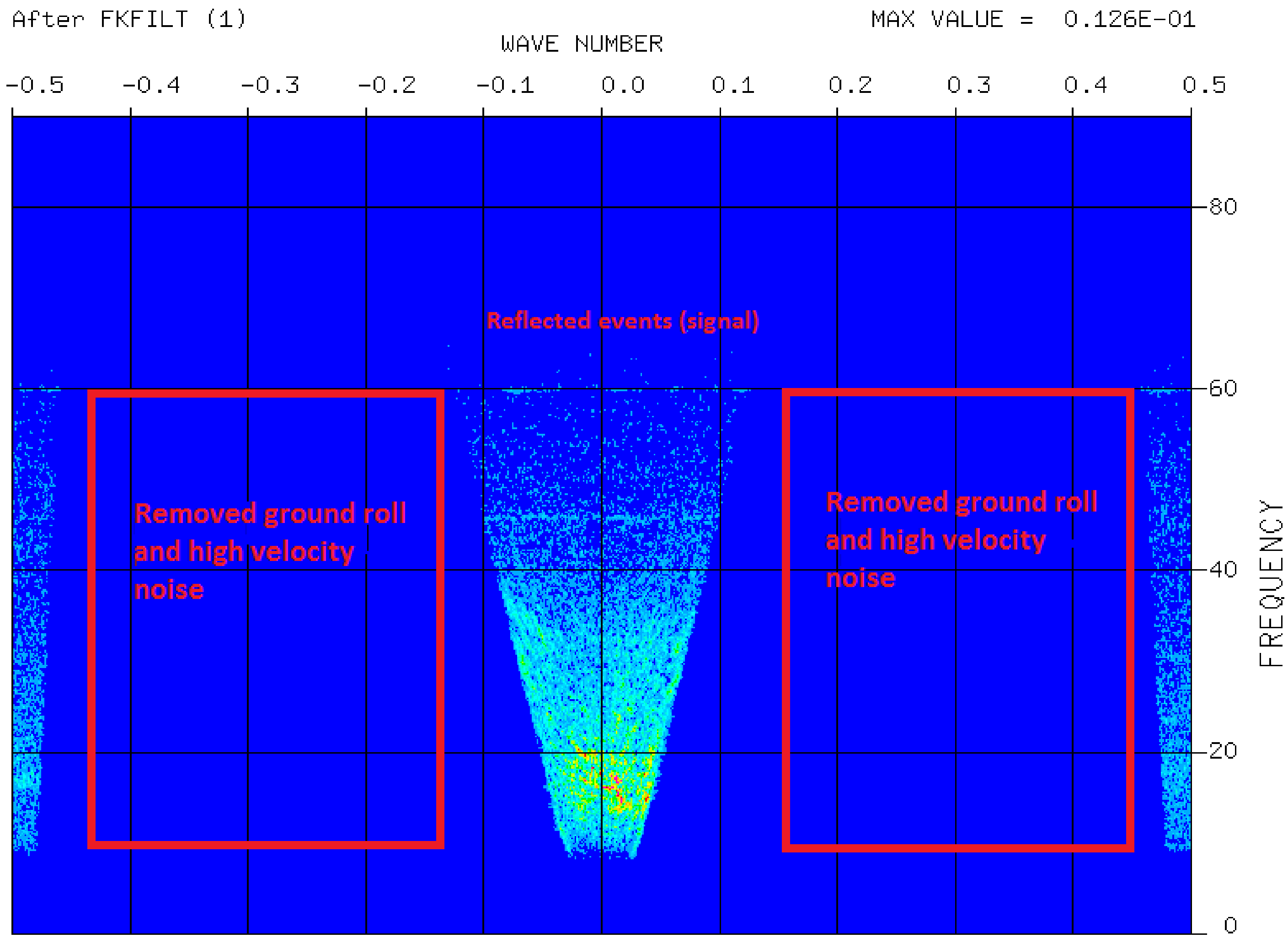

Figure 2.17. F-K spectrum after the F-K filtering. The high velocity noise and ground rolls are removed.

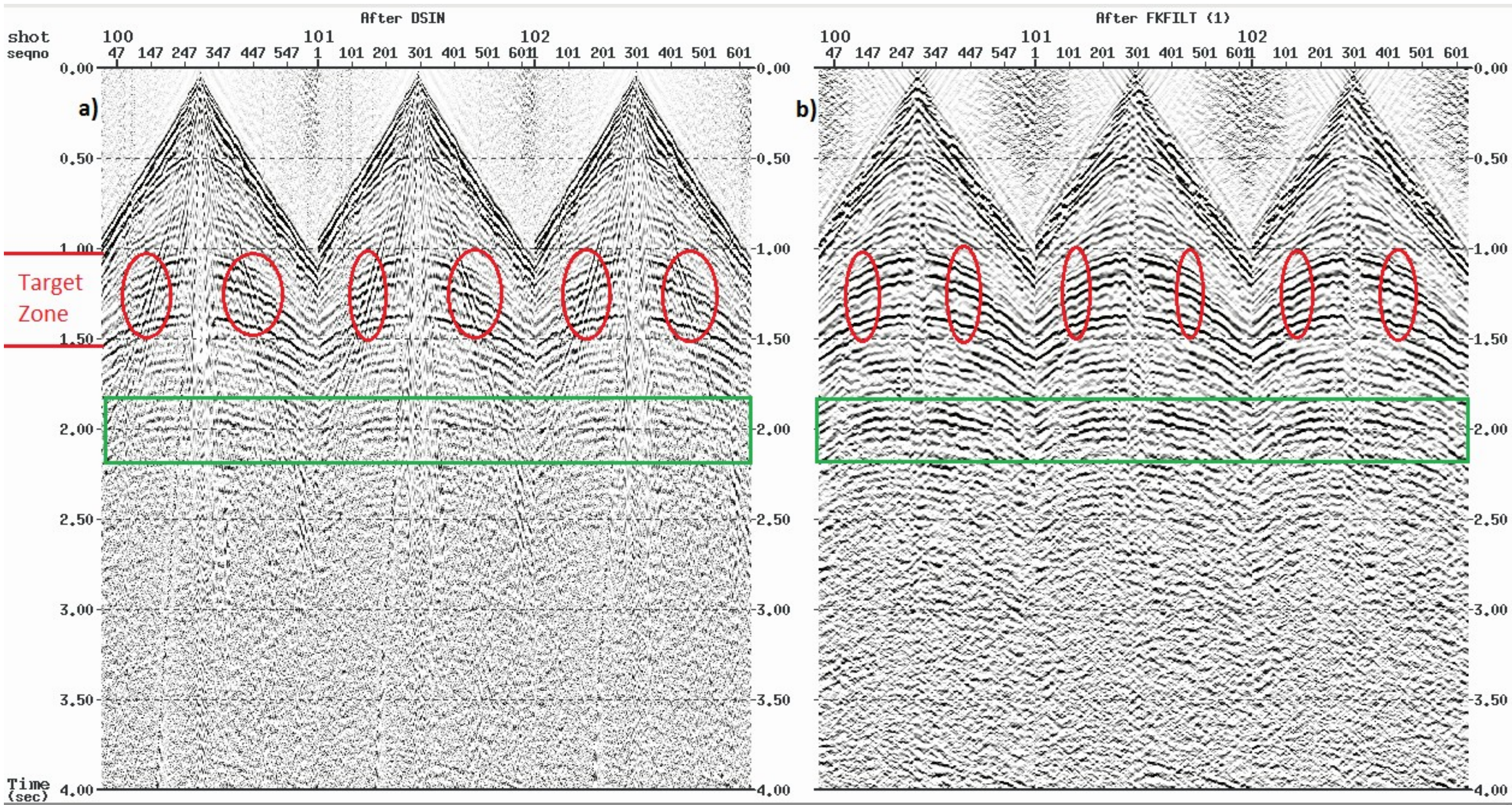

Figure 2.18. Represantative shot gathers from 100 to 102. a) Shot gathers before band-pass filtering. b) The same shot gathers after noise attenuation. The obtained results indicate that the noises are suppresed, and the reflections are stronger notably.

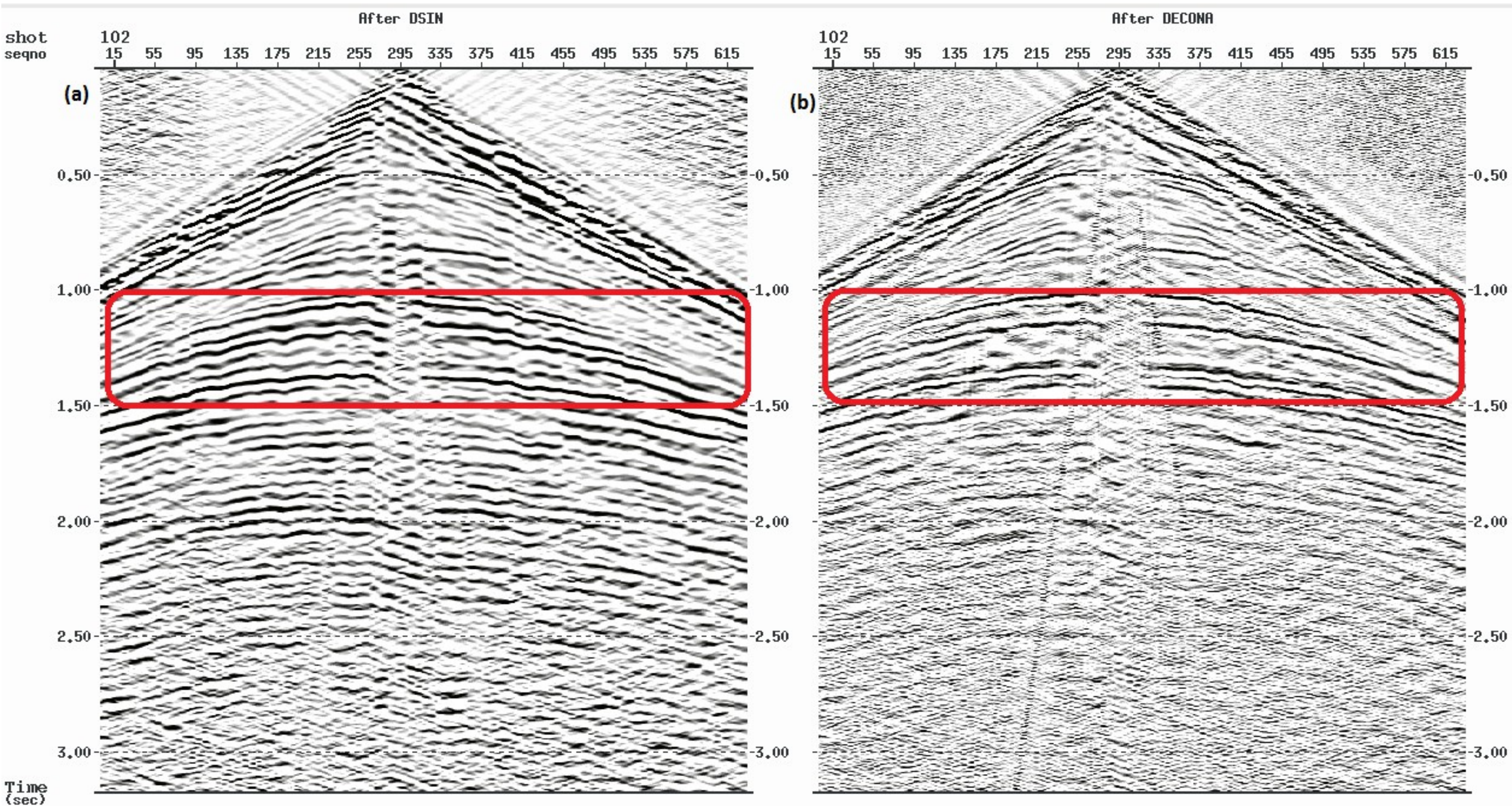

Figure 2.19. Shot gather 102. a) Before the spiking deconvolution. b) After the spiking deconvolution. Seismic events are sharper after the spiking deconvolution.

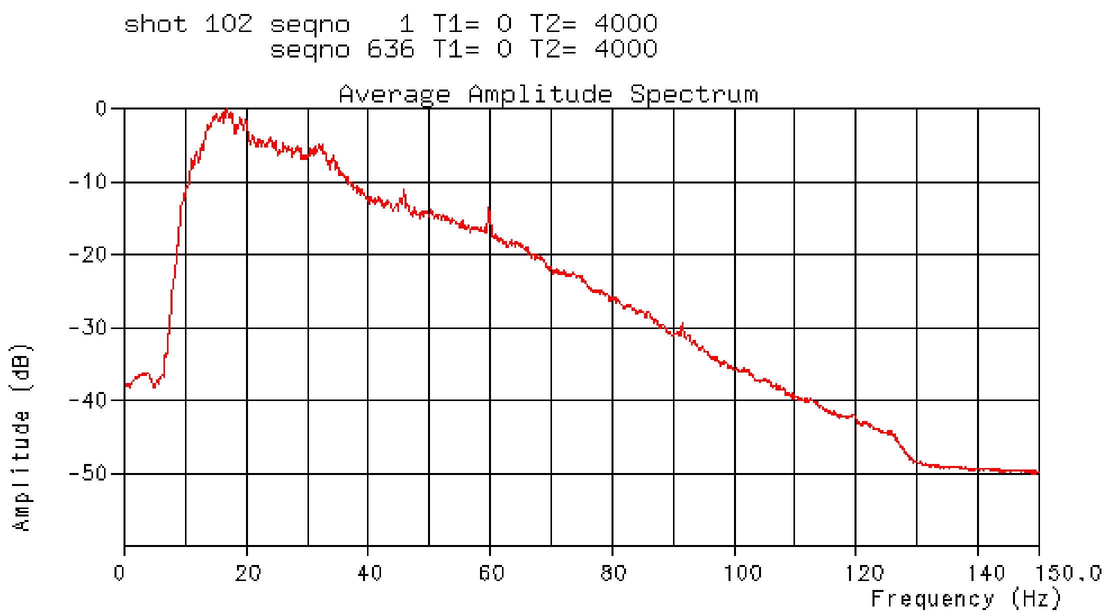

Figure 2.20. Amplitude spectrum of the shot gather 132 before the spiking deconvolution.

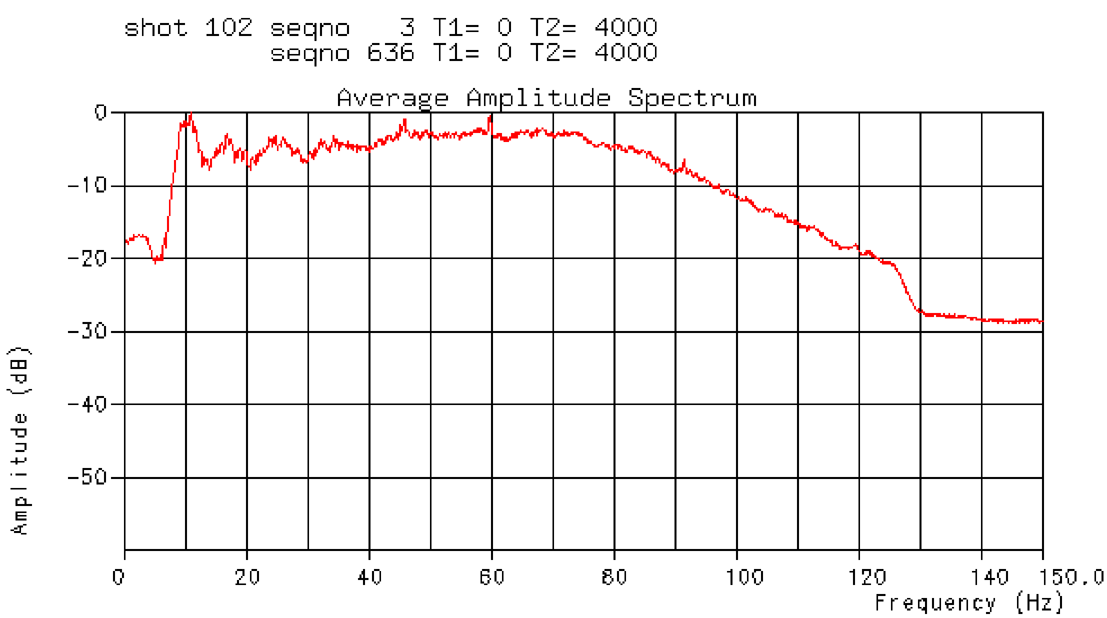

Figure 2.21. Amplitude spectrum of the shot gather 132 after the spiking deconvolution applied.

Until this stage, static corrections, noise attenuation, and deconvolution were applied to data. Stacked sections were obtained for before (Figure 2.22) and after (Figure 2.23) deconvolution in order to determine the quality of data for further processing steps. The obtained stacked sections show that the quality of the data are good to continue for further processing steps because seismic reflections are clear and strong at the target area, which is between 1300 ms and 1400 ms. Additionally, the area near the subsurface shows significant improvement.

2.6. VELOCITY ANALYSIS AND NORMAL MOVE-OUT (NMO) CORRECTION

Seismic velocity plays a key role in seismic processing and interpretationo. The accuracy of picking velocity is a fundamental parameter. Stacking, normal move out (NMO) corrections, time-to-depth conversion, and migration are related to seismic velocity, so the accuracy of velocity picking is vital for further processing steps (Qin et al., 2009). The seismic velocity is considered as a function of depth and vertical travel time, which are related to the computation of depths and displacements (Kaufman, 1953). Additionally, various velocity types can be used for several purposes and computed in different ways such as interval, average, NMO, RMS, stacking, and Dix velocity.

Porosity, density, pressure, and temperature are some main factors that influence the seismic velocities. Porosity has the highest effect on seismic velocity. Seismic velocity is also affected by frequency of seismic energy source and fractures in the subsurface (Yilmaz, 2001).

After deconvolution, the velocities from seismic data are designated in this study. The velocities obtained from seismic data give the best stack. NMO processing is crucial for picking velocities in order so that reflections are lined up in CMP gathers (Yilmaz, 2001). Velocity should have the correct value for acquiring flat reflections. If the velocity is low or high, the reflections overcorrected or undercorrected respectively (Figure 2.24).

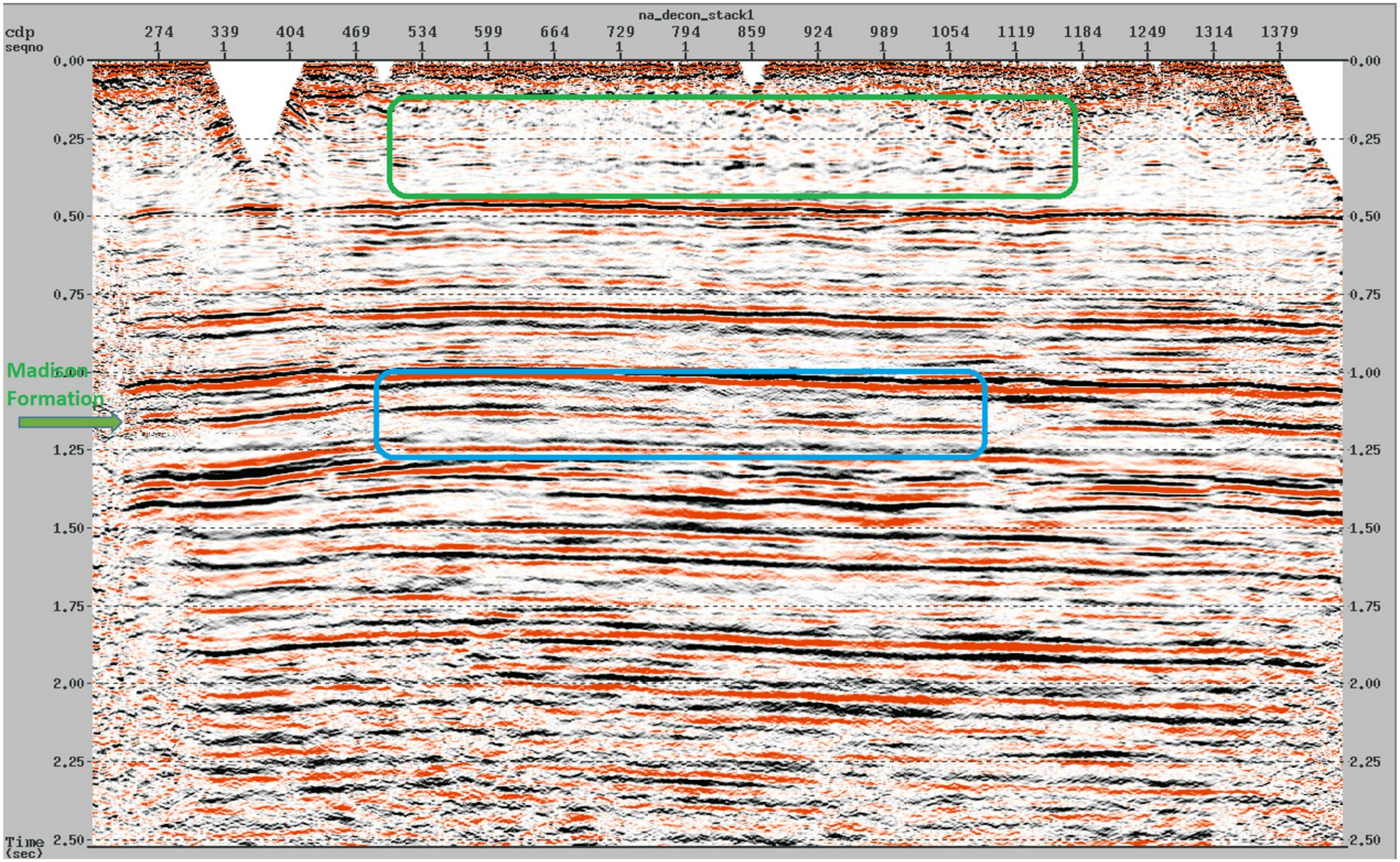

Figure 2.22. Stacked section before the spiking deconvolution.

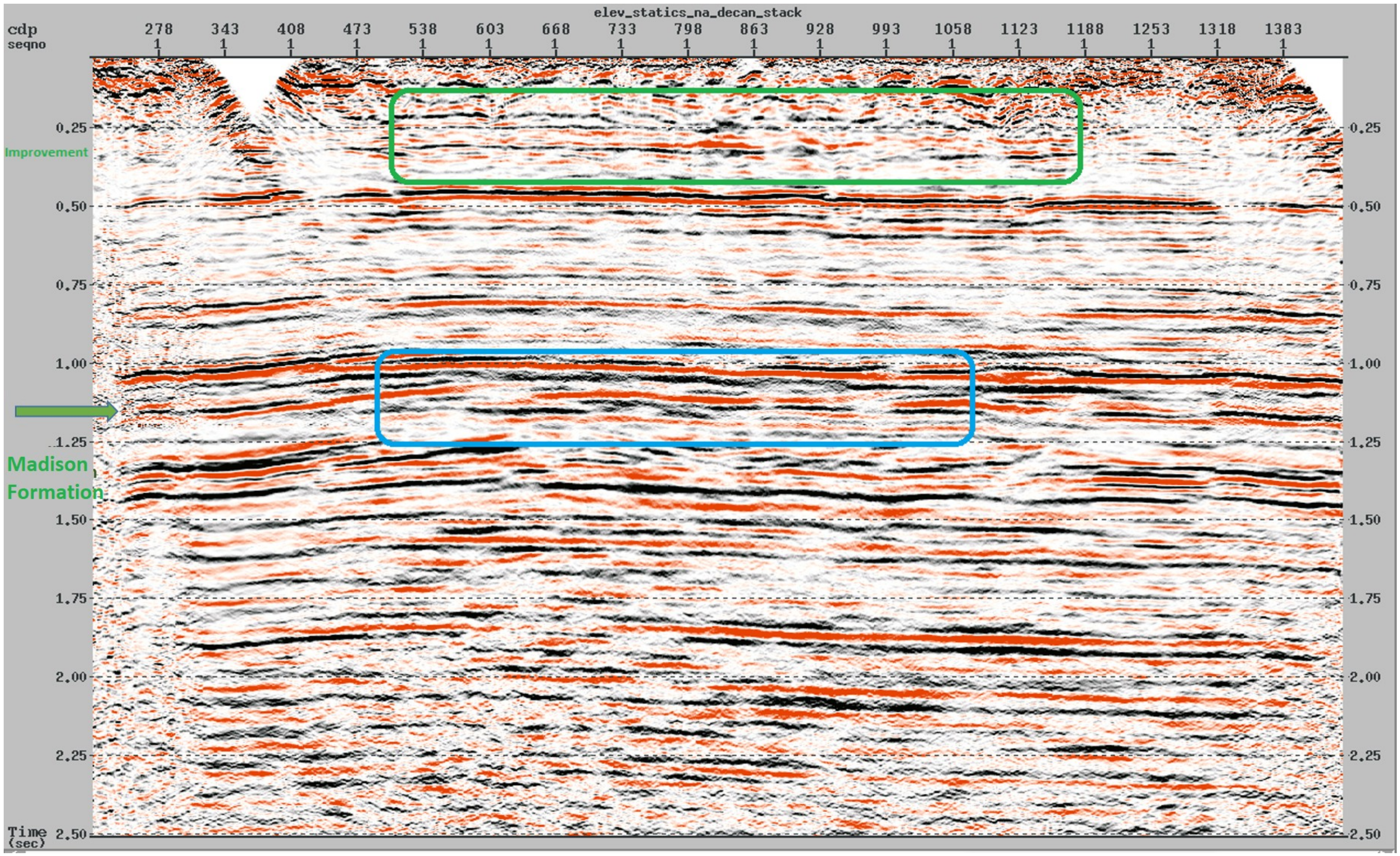

Figure 2.23. Stacked section after the spiking deconvolution. The areas show improvement.

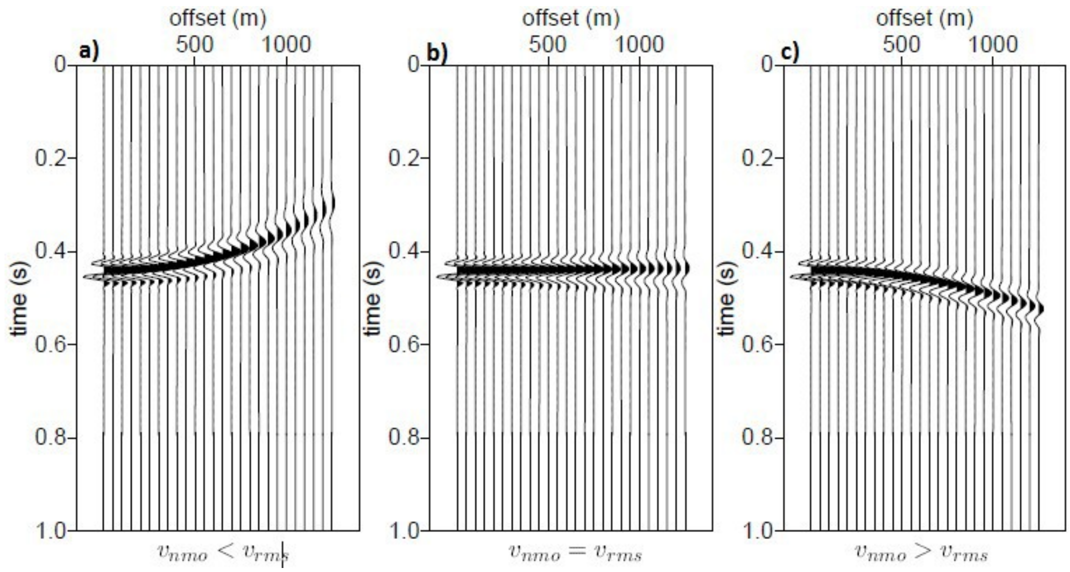

Figure 2.24. CMP gather showing reflection. a) With low velocity. b) Correct velocity. c) High velocity (Drijkoningen and Verschuur, 2003).

Number of traces, spread length, frequency bandwidth of seismic source, and spread length are some factors that have impacts on the resolution and accuracy in velocity analysis. In this step, pre-stack deconvolution is used to seismic data in order to enhance the resolution, which assists to have higher velocity resolution in the velocity spectrum (Yilmaz, 2001).

There are several velocity analysis techniques which include the following:

1. Constant velocity panels (CVP)
2. Constant velocity stacks (CVS)
3. Analysis of velocity spectra
4. Barehole methods and VSP
5. (t2-x2) analysis

A velocity spectrum is generated before picking velocities. The conventional NMO semblance method is a common method to generate a velocity spectrum (Taner and Koehler, 1969). The principle is based on the NMO correction on selected CMP gathers over a velocity spectrum. In this study, the constant velocity stack and the semblance method were applied. Paradigm Echos, which is the software used in this study, has two different tools for velocity analysis (Figures 2.25 and2.26).

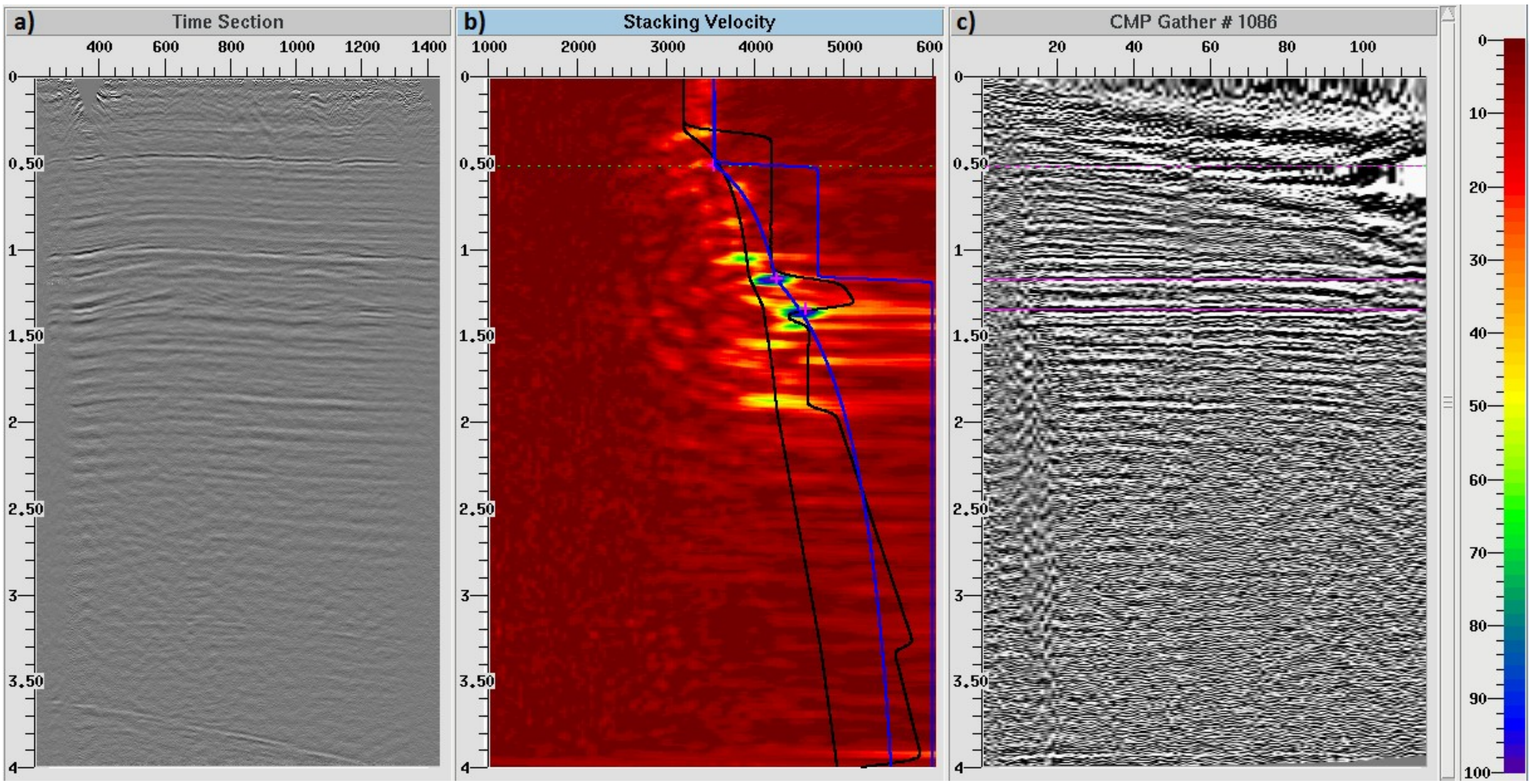

Figure 2.25. Velocity analysis tool. a) Stacked section. b) NMO semblance of CMP gathers. c) CMP gather 1086 to examine the changes of picked velocities for NMO and mute.

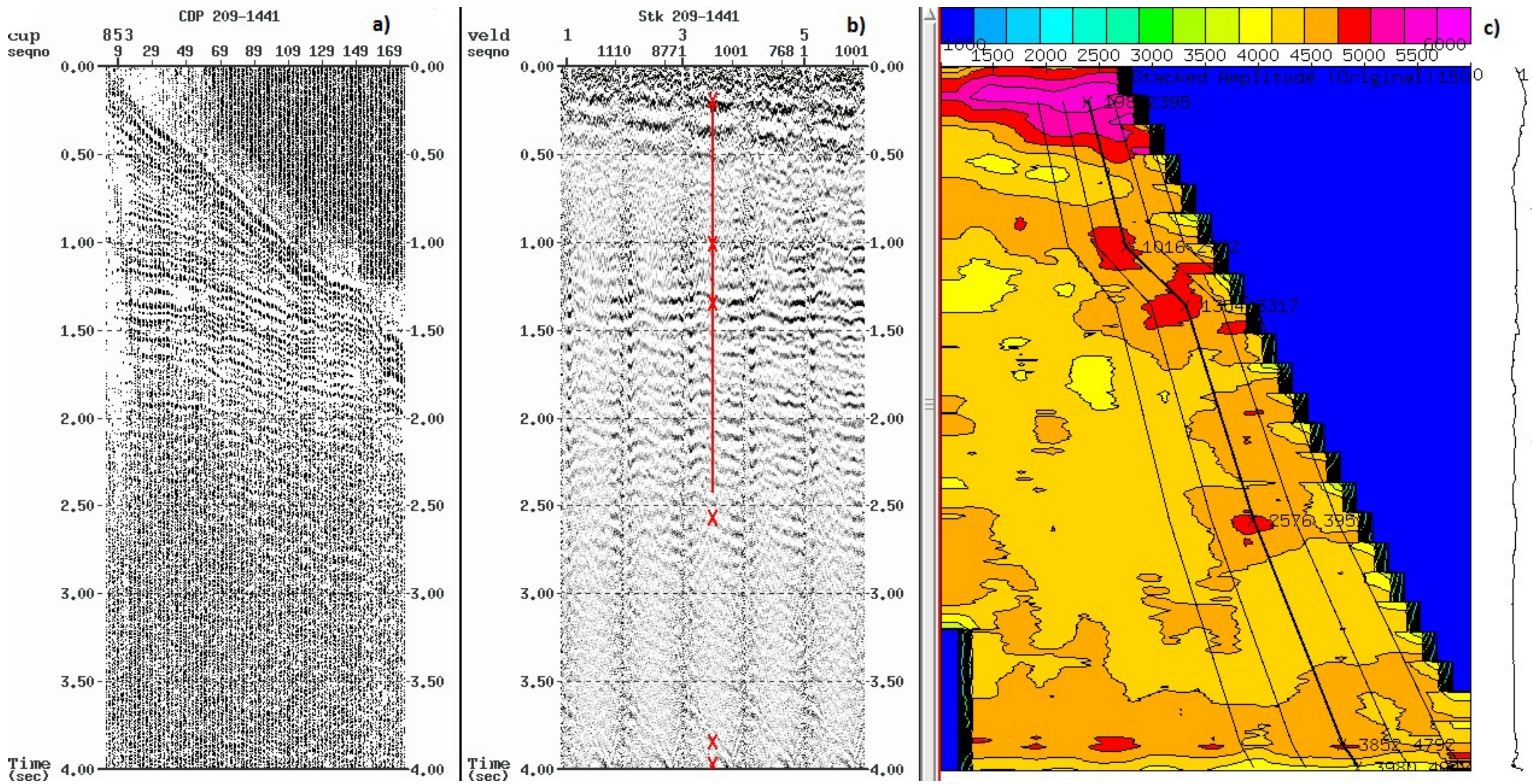

Figure 2.26. Velocity analysis tool. a) CDP gathers 209-1441. b) Obtained stacked section for the same CDP gathers. c) NMO semblance of the gathers. Higher amplitude areas are picked.

Figures 2.27 and 2.28 show before applying NMO and after applying NMO. The primary reflections of the seismic data were flattened which indicates that the velocities. They can be used to obtain the best quality stack.

2.7. RESIDUAL STATIC CORRECTIONS

Some reflections are influenced by very near surface conditions such as topography and velocity and the position of each shot and receiver. They cause short wavelength variations (small time shifts) for each trace. Correcting short wavelength time shifts is called residual static corrections (Pugin and Pullan, 2000). Also, near-surface velocity variations and inhomogeneity cause time anomalies, and these anomalies can be considered as surface consistent (Ronen and Claerbout, 1985). A surface-consistent model is applied in several seismic processing steps such as deconvolution and surface-consistent statics. Therefore, residual static corrections are crucial because they directly affect the quality of stack and migration section. Also, these corrections can be applied for processing both land and shallow marine data (Yilmaz, 2001). Applying the datum correction in the static correction stage is not enough to solve the near surface problem. Therefore, the residual statics are applied to seismic data before stacking to fix small time shifts and obtain better seismic data imaging (Faquan et al., 2011).

Residual static corrections are applied to seismic data without NMO. The iteration number of residual static corrections can differ based on the purpose of the study. After computing and applying iterations, velocity analysis is conducted again. This can help reanalyze the effect on the quality of the stacking section (Marsden, 1993).

In this study, two iterations of residual static correction were performed to the data. Figure 2.29 shows the stacked section before the residual statics. Figure 2.30 represents the horizontal display after the residual static corrections. After applying residual static corrections, reflections were stronger. The Madison Formation became more visible.

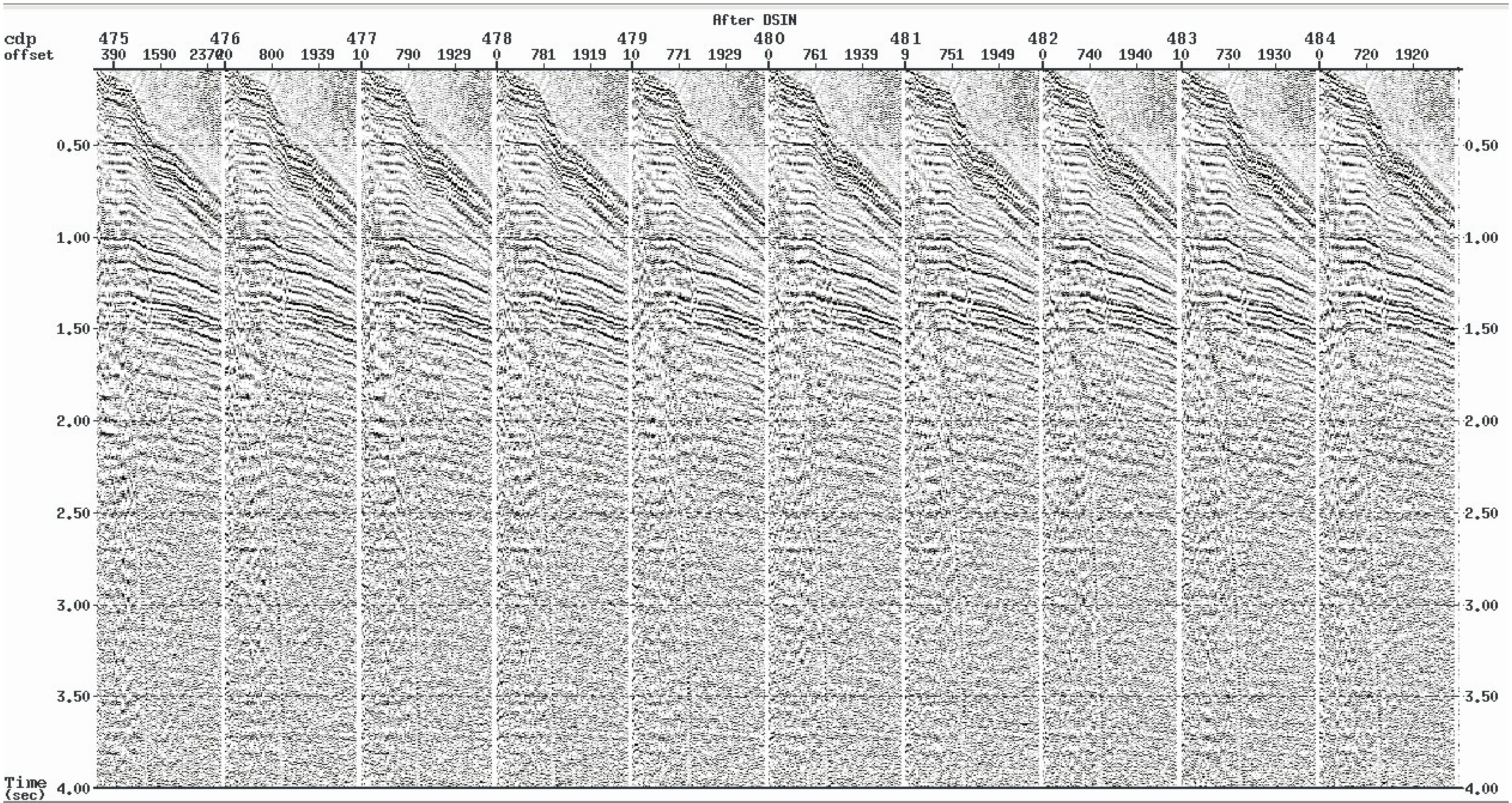

Figure 2.27. Several selected gathers 475-485 before applying NMO.

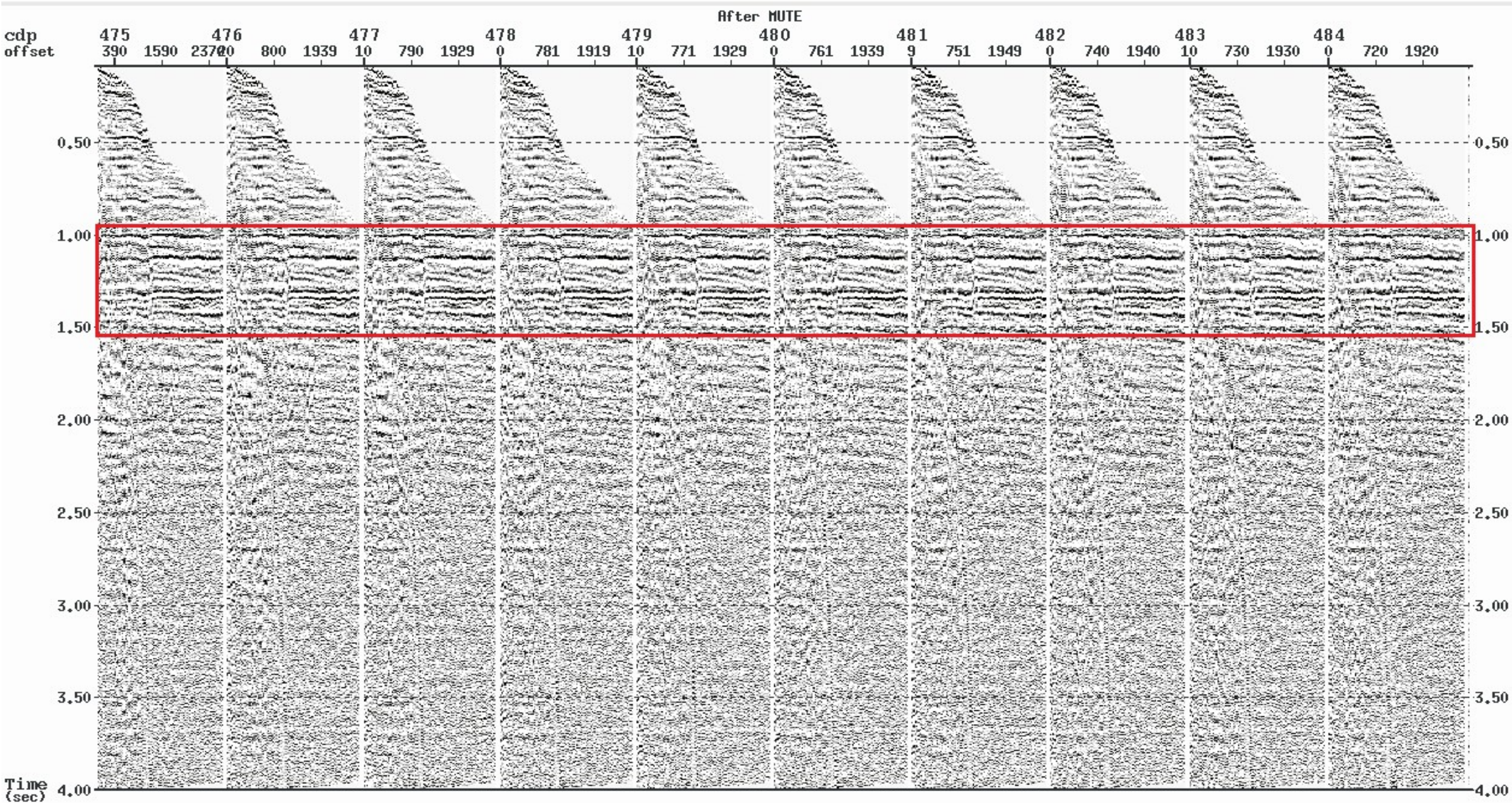

Figure 2.28. The same gathers 475-485 after applying NMO. The primary reflections are flattened.

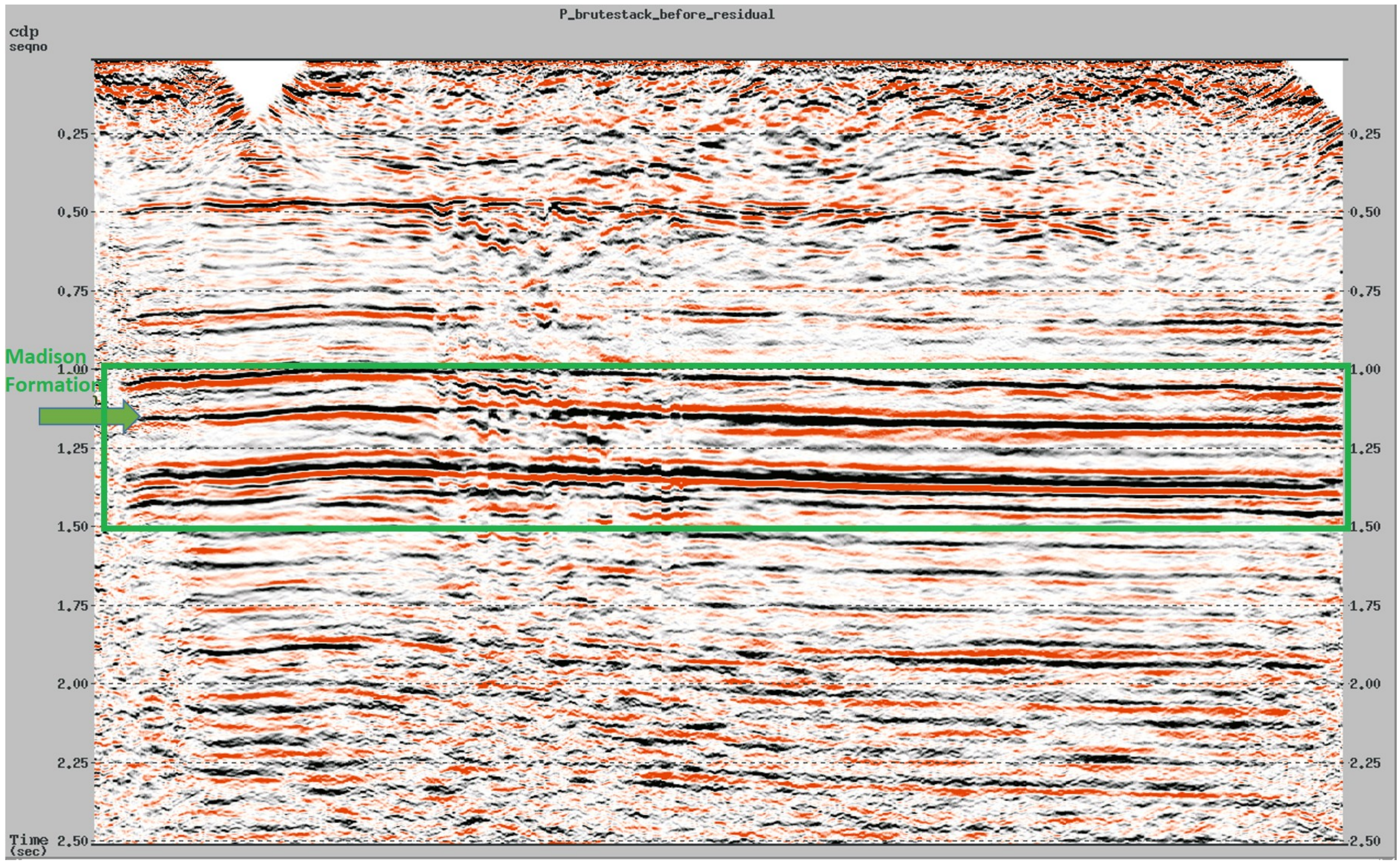

Figure 2.29. Stacked section before applying the residual statics.

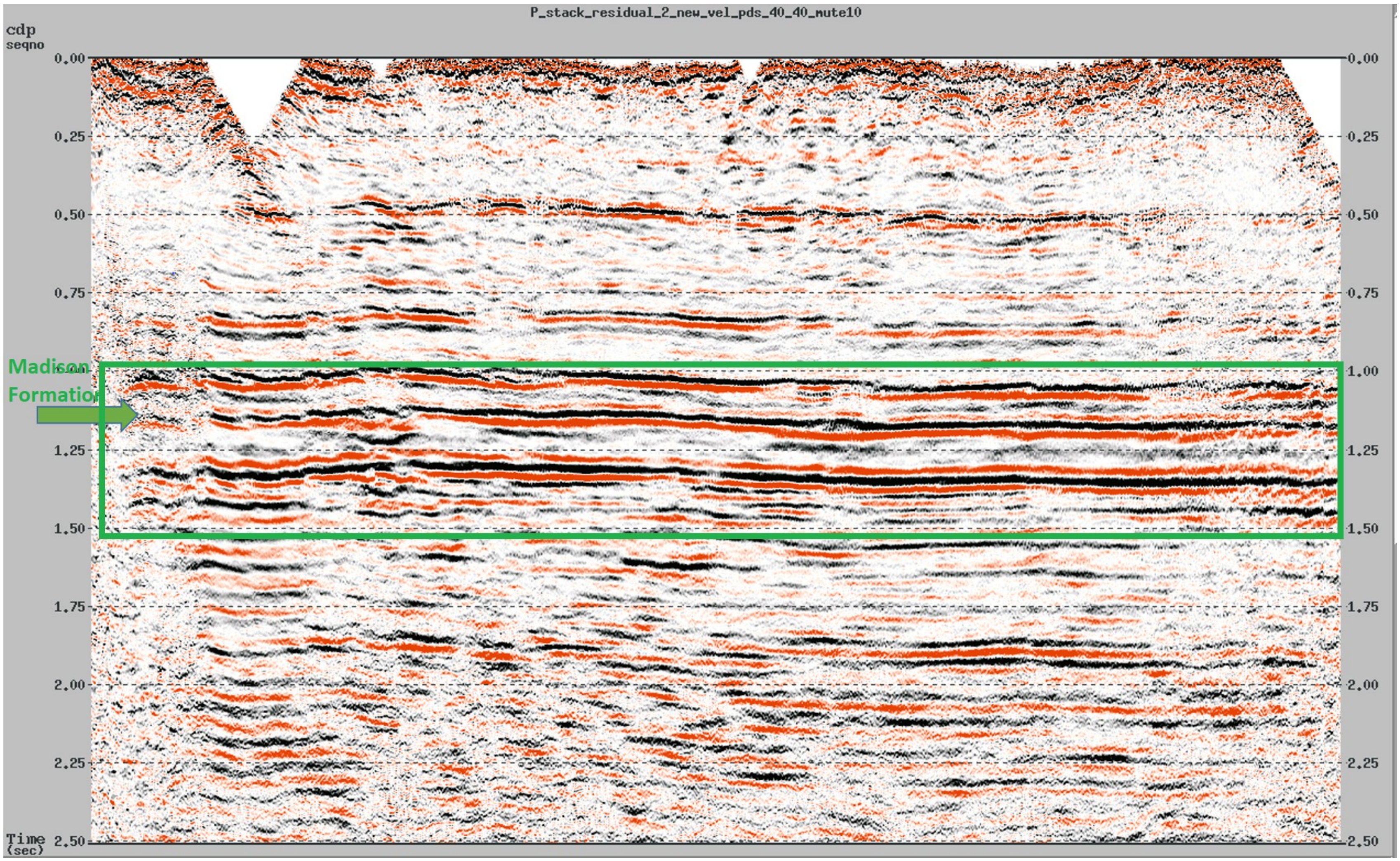

Figure 2.30. Stacked sections after the residual static corrections. The quality of the reflections have been improved.

2.8. STACKING

Stacking is combining traces from different records with a common depth point (CDP). Seismic data processing includes three crucial techniques, which are deconvolution, stacking, and migration (Figure 2.31) (Yilmaz, 2001). The main purpose of stacking is to minimize the noise and improve the quality of seismic data in the offset direction. Stacking is applied to traces after performing the NMO correction and then by compressing these in the offset domain.

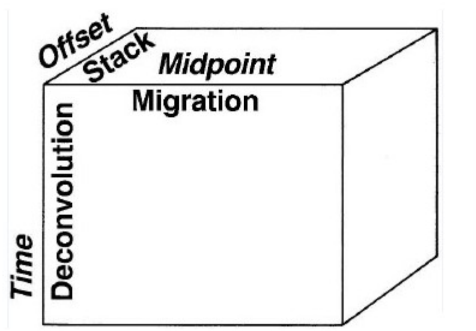

Figure 2.31. Three main steps in sesimic data processing (Yilmaz, 2001).

In general, floating datum, which is the smoothed version of the surface topography, is applied to seismic data. However, several migration algorithms are based on the horizontal plane (Zheng et al., 2000). In this study, after performing residual static corrections, a final stacking was permormed after applying NMO correction and picking velocities. Additionally, a floating datum stack gather and a flat datum stacked gather were obtained (Figures 2.32, 2.33, and 2.34). After applying flat datum, the data were shifted back to a flat datum, which is suitable to applymigration.

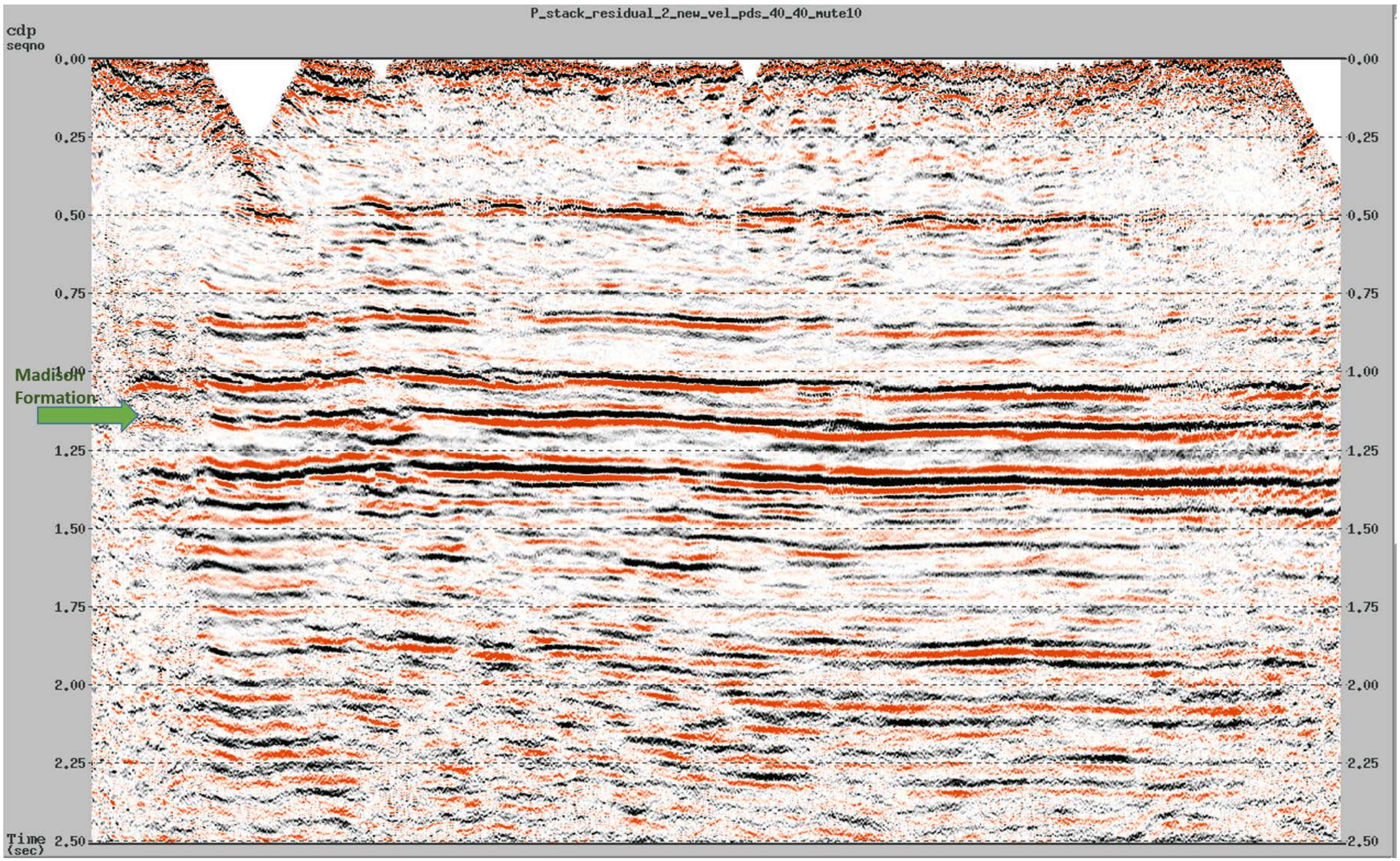

Figure 2.32. Stacked sections with floating datum.

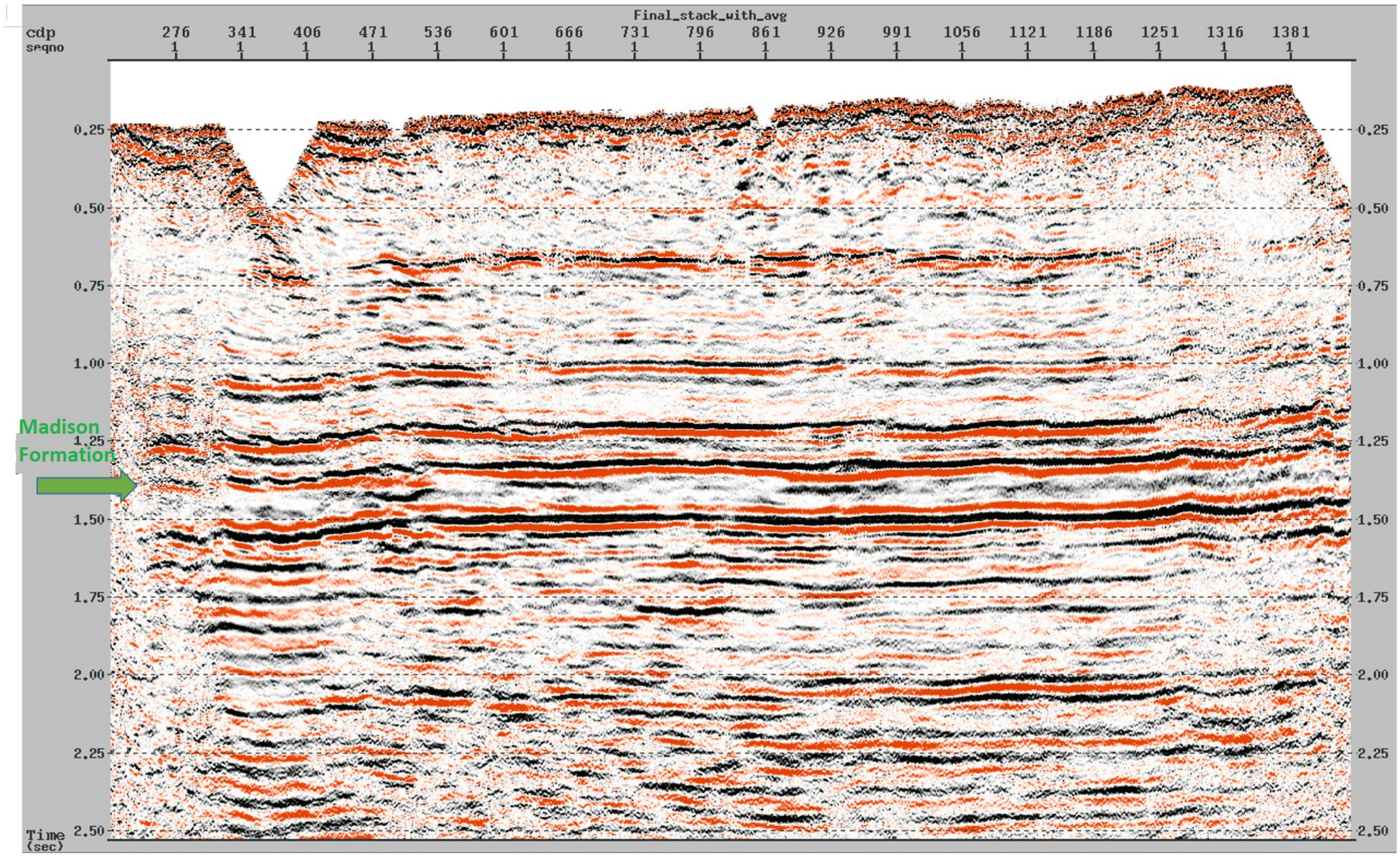

Figure 2.33. Stacked section corrected to a referance flat datum. The seismic data were moved back to a flat datum.

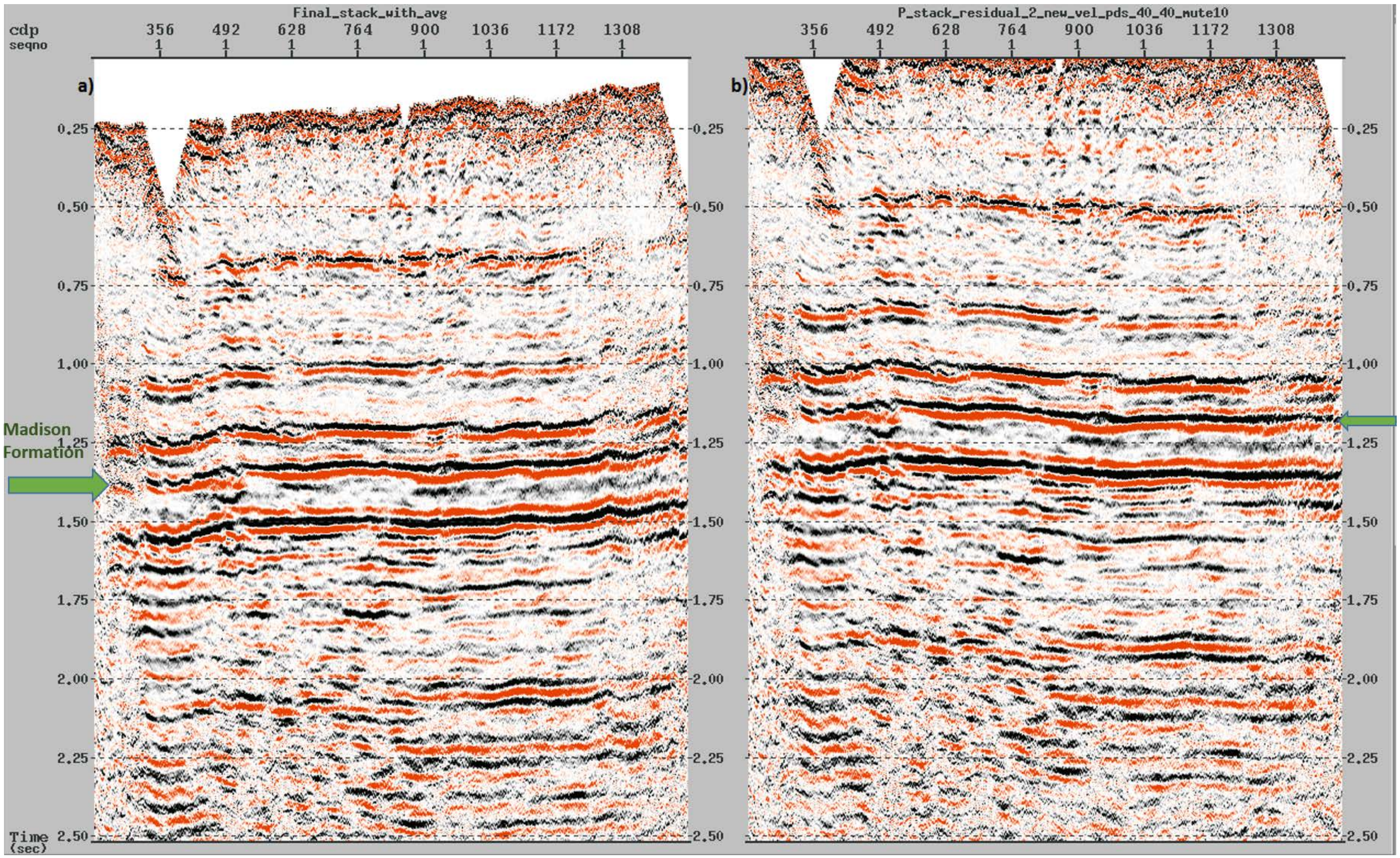

Figure 2.34. Stacked sections showing difference between flat datum and float datum. a). Stacked section with flat datum. b). Stacked section with float datum.

2.9. MIGRATION

Migration is one of the most important step of seismic data processing. It moves reflectors to their correct spatial and temporal positions, eliminates diffractions, and increases resolution. The main purpose of migration is to obtain the stacked gather which reflects the geologic cross section. There are several types of migration techniques in order to image the subsurface. These techniques contain (Yilmaz, 2001):

1. Time or depth migration
2. Prestack or poststack migration
3. Dimensionality, 2D or 3D

These migration techniques differ based on the nature of the subsurface. Therefore, the geology of the area plays a key role in order to determine which migration technique is suitable for the study area (Yilmaz, 2001).

Time migration is applied to produce a subsurface image since it is more efficient than depth migration. The other benefit of time migration is its lower sensitivity than depth migration (Dell et al., 2012). Beside, depth migration is used for complex velocity structures such as salt domes, near fault shadows, and thrust belts (Hill, 2001).

Prestack migration is generally used for complex geological structures because the common midpoint stacking fails. For complex geological structures, common mid-point are not the same as the common reflection point (Bording and Lines, 1997). Thus, prestack migrations generally require a fairly uniform offset distribution to be effective. On the other hand, the poststack migration is a partial prestack time migration. It has weaker sensibility to velocity. The Poststack migration is also cheaper than the prestack migration (Yilmaz, 2001). Several migration algorithms are used today. Cost, maximum dip to migrate, and frequency content of seismic data are key factors to decide which migration type is suitable to get the best result for seismic data. Generating an extrapolated seismic wavefield and moving reflectors to correct positions by using extrapolated seismic wavefield are two steps for migration methods working (Zhou, 2014).

In this study, 2D Kirchhoff time migration was applied to obtain the subsurface imaging. Two parameters, which are aperture width, also known as aperture migration, and maximum dip to migrate, affect the quality of Kirchhoff migration (Yilmaz, 2001). Kirchhoff migration is related to the diffraction accumulation approach. The aperture width is based on the amplitude summation (Rastogi et al., 2000). Maximum dip is the desired depth (in time) in the migration section.

In this study, poststack time migration was used to obtain the image of the target zone. Aperture width and maximum dip parameters were tested several times in order to acquire better imaging of the migration section (Figure 2.35). Figure 2.36 shows the result of the migration section with the target zone and target formation, which is the Madison Formation of the Mississippian Age. The formation was clearly shown on the final section of migration.

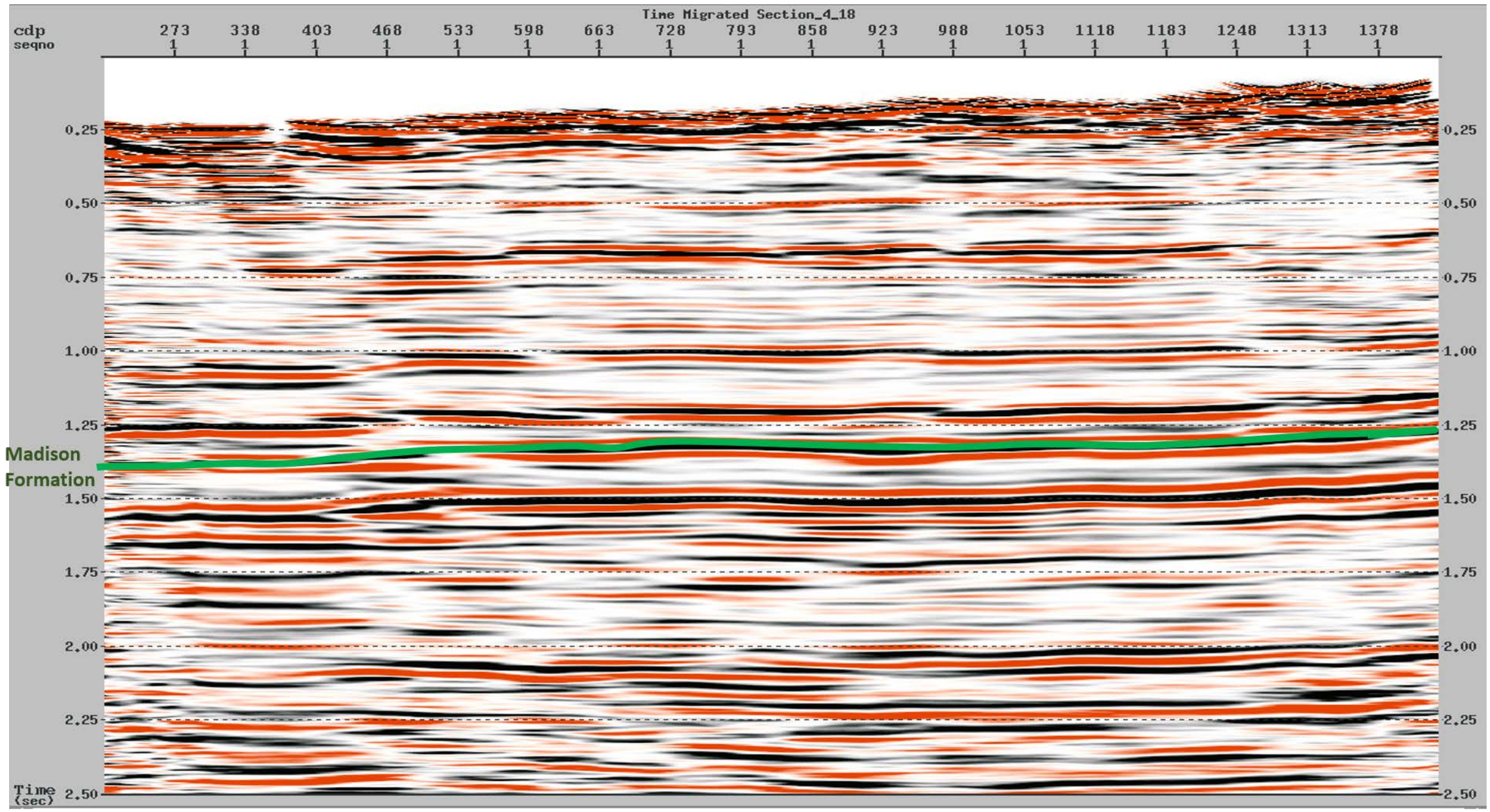

Figure 2.35. 2D Kirchhoff poststack time migrated section.

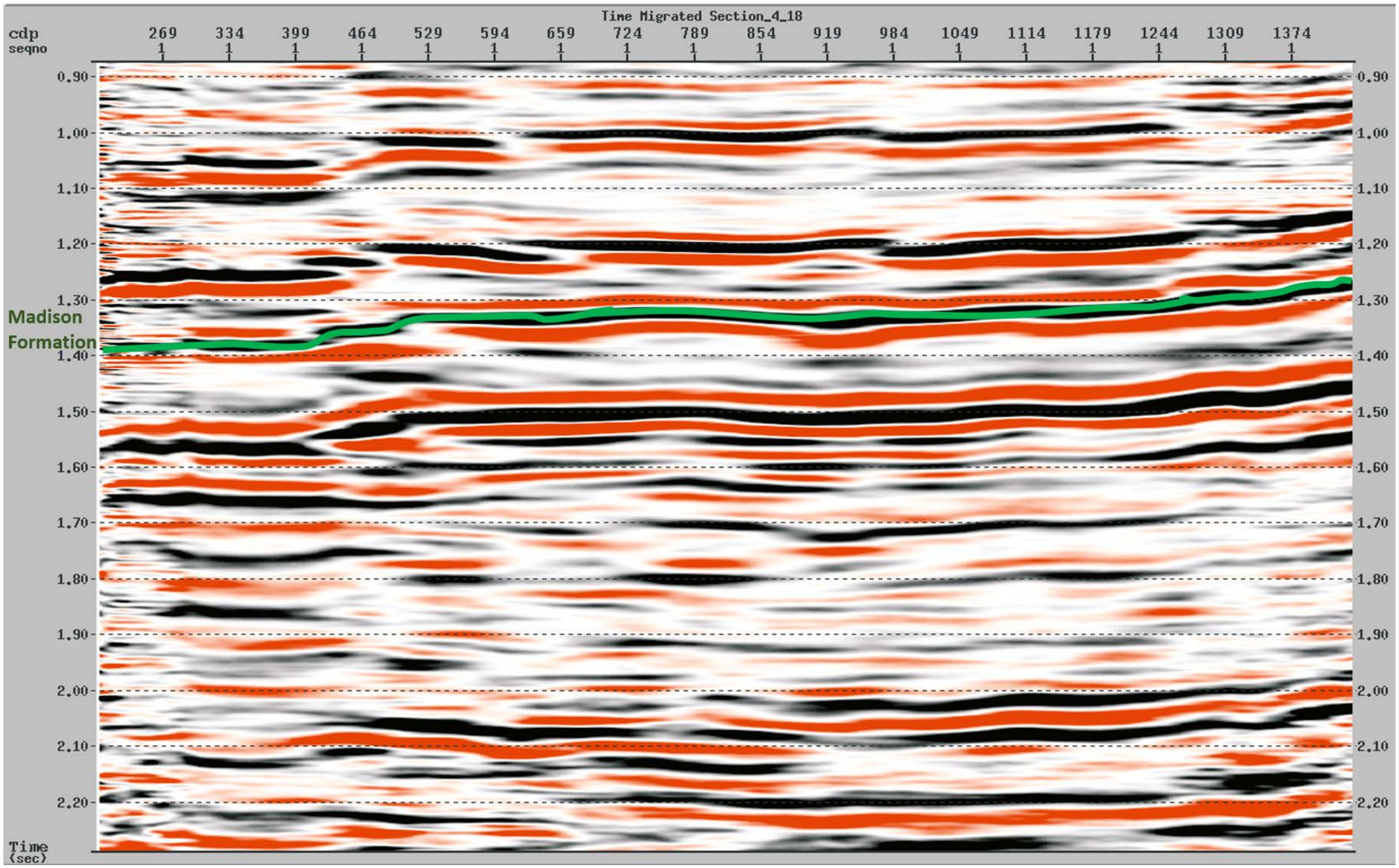

Figure 2.36. Same migrated sections with zoomed the Madison Formation.

3. CONCLUSIONS

The Spring Coulee 3C-2D seismic data Line 2008-SC-01 is reprocessed to obtain a better image of the subsurface and improve the quality of resolution of the Madison Formation, which is at between 1300 ms and 1400 ms.

The Echos software by Paradigm is used to process the seismic data. The seismic data is converted to the SEG-Y format from the SEG-D format. In the data, elevations of source and receivers are not correct, so these values are restored manually.

The first and second shots include strong noise, which can affect the quality of further processing steps. Therefore, they are omitted during the trace editing stage.

In order to remove the efeect of long wavelengths on the seismic data, elevation static correction are applied to the data.

AGC is applied to the data to improve the amplitude of the data. The data includes noises, such as ground rolls, high velocity noise, and air blast. To reduce the effect of these noises, band pass filtering, Supress module, and F-K filter are applied to the data. The results of applying band pass filtering show lowered air blast effect. After the Supress module, ground roll noises are reduced. Air blast and swell noises are omitted during this time. The data have strong ground rolls. In order to suppress ground rolls, F-K filtering is applied to the data. Several parameters are tested for each step on selected seismic gathers to decide which parameters give the best solution for the noise problem. Then, the chosen parameters are applied to the entire data. As a result of these steps, noises are removed significantly, and reflections are stronger.

Spiking deconvolution is performed on the data in order to acquire the temporal resolution of the data and enhance the frequency bandwidth. Before deconvolution, the frequency bandwidth is from 10 Hz to 35 Hz. After applying spiking deconvolution, this values enhance from 8 Hz to 95 Hz.

There are two different interactive tools used for velocity picking. Also, after velocity picking, mute and Normal Moveout (NMO) correction are applied to the data. After NMO correction, the reflections of the seismic data are flattened, which helps acquire the best quality stack.

Residual static corrections are used on the data to fix small time shifts (short wavelength) variations for each trace. Two iterations of residual static corrections are performed on the data in order to observe the improvement of reflections of the target area. After each iteration, velocity analysis is renewed because of the changing CMP gather. After each residual static correction, stacking is performed to analyze the improvement of the data. The results indicate that reflections are strong, and this stacked gather can be used for next processing steps.

Velocity analysis is renewed and Flat datum is applied to the data in order to obtain final stack gather to obtain final stacking gather, which is used for the migration.

In this study, 2D Kirchhoff poststack time migration is applied to the data. In order to obtain the best migration section, aperture width and maximum dip are selected many times. After deciding these parameters, the results show the quality and resolution of the target zone is significantly improved.

BIBLIOGRAPHY

Al Mukhtar, K. S. and Aswad, N. N. (2016). Application of the elevation and residual static correction methods on a selected seismic data of west Luhais area in the south of Iraq.

Bertram, M. B., Hall, W., Stewart, R. R., Gallant, E. V., Margrave, G. F., and Maier, R. (2008). Overview of multicomponent seismic field work at Spring Coulee, Alberta.

Bording, R. P. and Lines, L. R., 1997, Seismic modeling and imaging with the complete wave equation. Society of Exploration Geophysicists Tulsa.

Broadhead, M. K., Liner, C. L., Ulrych, T.J., et al. (2007). Predictive deconvolution by frequency domain wiener filtering. In 2007 SEG Annual Meeting. Society of Exploration Geophysicists.

Chen, Y., Jin, Z., Gan, S., Yang, W., Xiang, K., et al. (2015). Deblending using a combined pnmo-mf-fk coherency filter. In 2008 SEG Annual Meeting. Society of Exploration Geophysicists.

Chiu, S. K,. Howell, J. E., et al. (2008). Attenuation of coherent noise using localized adaptive eigenimage filter. In 2008 SEG Annual Meeting. Society of Exploration Geophysicists.

Connolly, C. A., Walter, L. M., Baadsgaard, H., and Longstaffe, F. J., 1990, Origin and evolution of formation waters, Alberta Basin, Western Canada sedimentary Basin. I. Chemistry: Applied Geochemistry, 5(4), 375–395.

Costain, J. K. and Coruh, C. (2004). Basic Theory in Reflection Seismology: with MATHEMATICA Notebooks and Examples on CD-ROM, volume 1. Elsevier.

Deere, J. (2009). Introduction to this special section-Statics. The Leading Edge, 28(2):190-191

Deighan, A.J. and Watts, D. R. (1997). Ground-roll suppression using the wavelet transform. Geophysics, 62(6):1896-1903.

Dell, S., Gajewski, D., and Vanelle, C., 2012, Prestack time migration by common-migrated-reflector-element stacking: Geophysics, 77(3):S73–S82.

Drijkoningen, G. and Verschuur, D. (2003). Seismic data processing (ta3600/tg001), centre for technical geoscience. Delft University of Technology, PO Box, 5028:2600.

Evans, B. J. and Dragoset, W. H. (1997). A handbook for seismic data acquisition in exploration. Society of Exploration Geophysicists.

Faquan, F., Yusheng, Z., City, B. Z., and Province, H. (2011). International geophysical conference, Shenzen, China, November 7-10, 2011.

Garland, J., Neilson, J., Laubach, S. E., and Whidden, K. J. (2012). Advances in carbonate exploration and reservoir analysis. Geological Society, London, Special Publications, (370):1-15.

Higley, D. (2013). Assessment of undiscovered conventional oil and gas resources of the Western Canada sedimentary Basin, Canada, 2012. Technical report, US Geological Survey.

Hill, N. R. (2001). Prestack gaussian-beam depth migration. Geophysics, 66(4):1240-1250.

Kaufman, H. (1953). Velocity functions in seismic prospecting. Geophysics, 18(2):289-297.

Kearey, P., Brooks, M., and Hill, I. (2013). An introduction to geophysical exploration. John Wiley & Sons.

Kent, D. and Kreis, L. (2001). Mississippian Madison formation low-gravity oilfields in southwestern Saskatchewan: Examples of unconformity diagnesis controlling reservoir quality. Summary of Investigations by the Saskatchewan Geological Survey, 1:46.

Lauren, O. A. and Stewart, R. R. (2008). An integrated geological and geophysical analysis of the hydrocarbon potential of the Spring Coulee, Alberta area. Technical report, CREWES Research Report.

Lee, M. W., Agena, W. F., Grow, J. A., and Miller, J. J. (1999). Seismic processing and velocity assessments. The oil and gas resource potential of the 1002 Area, Arctic National Wildlife Refuge, Alaska: US Geological Survey Open-File Report, pages 98-34.

Leinbach, J. (1995). Wiener spiking deconvolution and minimum-phase wavelets: A tutorial. The Leading Edge, 14(3): 189-192.

Li, P., Feng, Z., Li, Z., Zu, Y., and Hou, X. (2006). Static correction technology and applications in comple areas of Western China. The Leading Edge, 25(11):1384-1386.

Liu, B. et al. (1997). Evolution of fluid flow systems, geothermal regime, and hydrocarbon migration and accumulation in the Alberta basin. Proc. 308 Int’l. Geol. Cong, 8:222-241.

Lu, H.-x. and Hall, K. W. (2008). Preliminary processing results, Spring Coulee, Alberta. CREWES Research Report, page 20.

Marsden, D. (1993). Static corrections-A review, part iii. The Leading Edge, 12(3):210-216.

Ostridge, L. A., Lawton, D, C., and Stewart, R.R. (2009). Spring Coulee seismic interpretation.

Pokhriyal, S., Nautiyal, A., Gupta, O., et al. (1992). New algorithm for automatic editing of noisy seismic data. In 1992 SEG Annual Meeting. Society of Exploration Geophysicists.

Pugin, A. and Pullan, S. E. (2000). First-arrival alignment static corrections applied to shallow seismic reflection data. Journal of Environmental & Engineering Geophysics, 5(1):7-15.

Qin, L., Hong, F., Qingchun, L., et al. (2009). Method of seismic interactive velocity analysis.

Rastogi, R., Yerneni, S., and Phadke, S. (2000). Aperture width selection criterion in Kirchhoff migration. In Association of Exploration Geophysicists Seminar on Exploration Geophysics, Goa, India.

Ronen, J. and Clearbout, J. F. (1985). Surface-consistent residual statics estimation by stack-power maximization. Geophysics, 50(12):2759-2767.

Sheriff, R, and Geldart, L. (1983). Exploration seismology. Volume 1: History, theory, and data acquisition.

Sheriff, R. E. (2002). Encyclopedic dictionary of applied geophysics: Tulsa, Oklahoma. Society of Exploration Geophysicists.

Suarez, G. M. and Stewart, R. R. (2008). Seismic source comparison for compressional and converted-wave generation at Spring Coulee, Alberta. Part i: Heavy vibroseis dynamite comparison. CREWES Research Report, 20.

Talagapu, K. K. (2004). 2d and 3d land seismic data acquisition and seismic data processing. MSc, Thec, India: Andhra University.

Taner, M. T. and Koehler, F. (1969). Velocity spectra-Digital computer derivation applications of velocity funcitons. Geophysics, 34(6):859-881.

Ulrych, T.J. and Matsuoka, T. (1991). The output of predictive deconvolution. Geophysics, 56(3):371-377.

Velis, D. R. et al. (2006). Parametric sparse-spike deconvolution and the recovery of the acoustic impedance. In 2006 SEG Annual Meeting. Society of Exploration Geophysicists.

Wright, G., McMechan, M., Potter, D., Mossop, G., and Shetsen, I. (1994). Structure and architecture of the Western Canada sedimentary Basin. Geological Atlas of the Western Canada sedimentary Basin, 4:25-40.

Yao, Z., Margrave, G. F., and Gallant, E. V. (1999). Optimal time-delay spiking deconvolution and its application in the physical model measurement. Technical report, CREWES Research Report.

Yilmaz, O. (2001). Seismic data analysis: Processing, inversion, and interpretation of seismic data: SEG.

Zhang, W., Zhang, H., and Li, J. (2017). 2017 workshop: Microseismic technologies and applications, Hafei, China, 4-6 June 2017.

Zheng, Y. et al. (2000) Migration redatuming and velocity conversion. In 2000 SEG Annaul Meeting. Society of Exploration Geophysicists.

Zhou, H.-W. (2014). Practical seismic data analysis. Cambridge University Press.

Zhu, X., Gao, R., Li, Q., Guan, Y., Lu, Z., and Wang, H. (2014). Static corrections methods in the processing of deep reflection seismic data. Journal of Earth Science, 25(2):299-308.

VITA

Yasin Demir was born in Ankara, Turkey, in 1990. He graduated from Black Sea Technical University, in the department of Geophysical Engineering in June 2012. He had an internship at Turkish Petroleum Corporation (TPAO) in 2011.

He was awarded a scholarship from the Turkish Petroleum Corporation and completed his language program at the University of Texas at Arlington. He started his masters program at Missouri University of Science and Technology in August 2016 in Rolla, Missouri. He worked on the reprocessing of the 3C-2D seismic data from the Spring Coulee Field, Alberta during his studies. He received the Master of Science in Geology and Geophysics from Missouri University of Science and Technology in August2018.